

“Babeş-Bolyai” University, Cluj-Napoca

Faculty of Physics
&
Interdisciplinary Research Institute on Bio-Nano-Sciences

INVESTIGATION OF BIOLOGICALLY ACTIVE COMPOUNDS

PhD Thesis

Summary

Mureşan-Pop Marieta

Scientific coordinator:

Prof. dr. Simon Simion

February 2012

Content

Abstract.....	1
1 Introduction and motivation.....	3
1.1 Ambazone: Historic. Properties.....	3
1.2 Background information: Polymorphism. Salts. Cocrystals.	3
2 Solid forms. Methods of preparation and investigations	5
2.1 Methods of preparation of new solid forms and growth of single crystals	
Error! Bookmark not defined.	
3 Experimental procedure	6
3.1 Ambazone monohydrate and anhydrous	6
3.1.1 DTA-TGA analysis	7
3.1.2 Powder X-Ray Diffraction (PXRD).....	7
3.1.3 Variable Temperature Powder X-Ray Diffraction (VTPXRD)	8
3.1.4 Fourier Transformed Infrared Spectroscopy (FTIR).....	9
3.1.5 Solid state ¹³ C NMR Spectroscopic analysis	10
3.1.6 Scanning Electron Microscopy SEM	10
3.1.7 Crystal structure determination from X-ray Single-crystal diffraction.....	10
3.2 Ambazone acetate.....	13
3.2.1 Powder X-Ray Diffraction (PXRD).....	13
3.2.2 DTA-TGA analysis	14
3.2.3 Variable temperature powder X-ray diffraction (VTPXRD).....	16
3.2.4 Fourier Transformed Infrared Spectroscopy (FTIR).....	16
3.2.5 Crystal structure determination from X-ray Single-crystal diffraction.....	17
3.3 Ambazone hydrochloride	18
3.3.1 DTA-TGA analysis	18
3.3.2 Powder X-ray diffraction (PXRD)	19
3.3.3 Fourier Transformed Infrared Spectroscopy (FTIR).....	20
3.3.4 Solid state ¹³ C and ¹⁵ N NMR Spectroscopic analysis.....	20
3.4. Ambazone glutamate	21
3.4.2. Powder X-Ray Diffraction (PXRD).....	22
3.4.3. Fourier Transformed Infrared Spectroscopy (FTIR).....	22
3.4.4. Solid state ¹³ C RMN Spectroscopic analysis.	23
3.5. Ambazone p-Aminobenzoate	24

3.5.1. DSC, DTA-TGA analysis	24
3.5.2. Powder X-Ray Diffraction (PXRD).....	25
3.5.3. Fourier Transformed Infrared Spectroscopy (FTIR).....	25
3.5.4. Solid-state ¹³ C NMR Spectroscopic analysis	26
3.6. Ambazone aspartate.....	27
3.6.1. DTA-TGA analysis	27
3.6.2. Powder X-Ray Diffraction (PXRD)	28
3.6.3. Powder X-ray diffraction with variable temperature (VTPXRD).....	28
3.6.4. Fourier Transformed Infrared Spectroscopy (FTIR).....	29
3.6.5. Solid state ¹³ C NMR Spectroscopic analysis	30
3.7. Ambazone nicotinate	31
3.7.1. DSC, DTA-TGA analysis	32
3.7.2. Powder X-Ray Diffraction (PXRD)	33
3.7.3. Fourier Transformed Infrared Spectroscopy (FTIR).....	33
3.8. Ambazone lactate	34
3.8.2. Powder X-Ray Diffraction (PXRD)	35
3.8.3. Fourier Transformed Infrared Spectroscopy (FTIR).....	36
4. Conclusions, original contributions, results, perspectives	37
Selected references:	39

Keywords: Ambazone, solid forms, monocrystals, solvent drop grinding, slurry, vapor diffusion, vapor digestion, liquid diffusion, X-Ray variable temperature, X-Ray Single-Crystal Diffraction, FTIR.

ABSTRACT

The biologically active compound chosen for this study is an antimicrobial substance named Ambazone. This compound belongs to the class of antimicrobial drugs, is the active compound in Faringosept and is used frequently in local treatments of oral and pharyngeal cavity. Ambazone was less characterized in terms of structural properties and of the possibility of formation of new solid forms. It's known that solid forms include polymorph, solvates, salts, hydrates and co-crystals. Solid forms can greatly improve active compound in terms of solubility, bioavailability and dissolution rate. This study is mainly aimed to obtain as many Ambazone solid forms and their characterization in structural terms. The need to obtain solid forms of Ambazone result from the fact that it is very slightly soluble in water and solid forms of Ambazone can help to increase the solubility and thus to improve the quality of this pharmaceutical compound.

The thesis is structured in three chapters, ending with general conclusions and perspectives. The first chapter deals with the physical-chemical and pharmaceutical properties of Ambazone. The second chapter contains a brief overview of methods for obtaining and characterization of solid forms and single crystals growth. Also, in this section the investigation methods for solid forms obtained from powders and single crystals are presented: thermal methods (DSC, DTA-TGA), spectroscopic techniques (FT-IR, solid state NMR) and diffraction methods (powder and X-ray single crystal diffraction). In Chapter 3 are presented the results obtained for the Ambazone based compounds obtained in this study. Starting from Ambazone monohydrate, we obtained the anhydrous form of Ambazone by using different preparation methods. Also, for both monohydrate and anhydrous Ambazone, we were able to obtain single crystals by Liquid Diffusion (LDif) preparation method, and therefore, a complete characterisation of their crystal structure was possible by single X-ray diffraction. Furthermore, there were established the conditions of conversion between the two monohydrate and anhydrous forms of Ambazone.

Another approach was to apply different preparation methods to obtain new forms from Ambazone mixed with acetic acid. We were able to achieve three different forms by Solvent Drop Grinding (SDG), Slurry (SL) and Vapor Digestion (VDig), and single crystals by Vapor Diffusion (VDif) method. All these compounds were characterized by the techniques mentioned in Chapter 2. The solvent drop grinding method was further used in

combination with different compounds (hydrochloric acid, glutamic acid, aspartic acid, p-Aminobenzoic acid, nicotinic acid and lactic acid) and new Ambazone forms were obtained.

The structural investigation revealed that all the obtained compounds are salts. This issue is of great importance for the pharmaceutical industry, taking into account that salts have higher solubility, higher dissolution rate and show an increase of bioavailability, compared with the pure Ambazone. Hence, investigation of solubility, dissolution rate, stability and bioavailability of all these salts can follow the present work, to evaluate the obtained compounds as potential application in the pharmaceutical industry.

CHAPTER 1

1 Introduction and motivation

1.1 Ambazone: Historic. Properties.

The biologically active compound chosen for this study is an antimicrobial substance named ambazone. This is the active compound of Faringosept or drug, having the aspect of a dark-brown microcrystalline powder; it is odorless and tasteless powder, used for local treatment of bucofaringian cavity and antineoplastic cure, also. The latest studies on ambazone had revealed the fact that it has an antibacterial spectrum similar to that of sulphonamides [Löber *et al* 1989] [Löber *et al* 2007]. Investigations regarding ambazone in 1990 have described some antineoplastic properties and have shown that does not provide mutagenic effects, unpleasant reactions as other oncostatic drugs drugs [Kuhnel *et al* 1988a, Kuhnel *et al* 1988b, Baumgart *et al* 1988, Amlacher *et al* 1990, Gutsche *et al* 1990]. Although discovered in 1950's by Domagk, it is less characterized from the point of view of its structural properties and formation of new solid forms possibility. The requirement of obtaining and characterizing of solid forms derives from the improvement they can bring to the properties of drugs' active compound regarding the solubility, biodisponibility and dissolving speed. For ambazone there were not reported new solid forms and its crystal and molecular structure was determined only from powder diffraction data and reported in the international conference Nanospec 2008 [Mocuta *et al* 2008]. The new solid forms of ambazone, which is very slightly soluble in water, can help to increase its solubility and thus to improve the quality of the pharmaceutical compound. The main purpose of this study was to obtain new solid forms of ambazone, to characterize their structure by various techniques, and single crystal molecular structure establishment of ambazone's and the new crystalline forms.

1.2 Background information: Polymorphism. Salts. Cocrystals.

In scientific terms “polymorphism” means the ability of a material – with the same chemical composition – to exist in different forms of crystalline structure, having different physical and chemical features, being a large interest phenomenon in pharmaceutical industry

[Bernstein 2002]. Worldwide, the researches of polymorphism and new solid forms are based on synthesis and physicochemical and structural characterization, in order to improve drug qualities and to reduce the side effects. Finding as much forms as possible has a major impact in the scientific field because different crystalline forms can generate a wide range of physical and chemical different properties which can affect the use of these materials. Solid forms include: polymorph (the same compound with different crystalline structure), solvates (in the compound's crystalline structure is included the solvent), hydrates (in the compound's crystalline structure are included molecules of water), salts or cocrystals which include in the crystalline structure two different compounds. The variety of solid forms which can be obtained for a compound is represented in Figure 1.1. It is possible to obtain salt when the difference between pK_a for the starting compound and pK_a of the compound that it combines with, is two units bigger. In this case a proton is transferred from acid to base. Co-crystals or „multi-component molecular crystals” [Bond 2007] are molecular structure which don't imply the establishment of some covalent bonds or proton transfer from the active compound.

Nevertheless, the physicochemical and pharmacological properties of cocrystals are different from those of the starting compound. Co-crystals have generally hydrogen bonds. For a long time, cocrystals were considered to be multicomponent crystals containing molecular units different from chemical point of view in asymmetrical unit [Etter *et al* 1993].

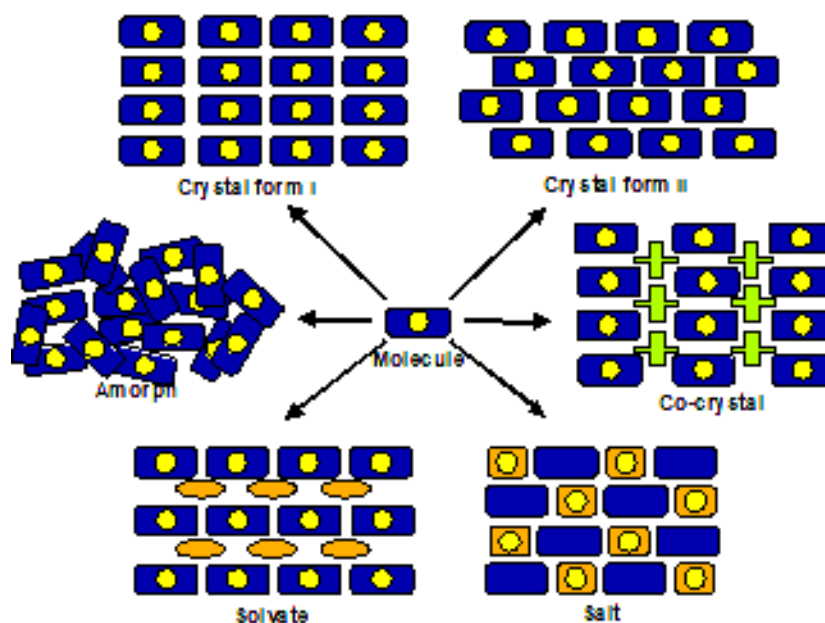


Figure 1.1. Schematic representation of the structural relationship between polymorphic (solvate, co-crystals, salts) and amorphous phases.

CHAPTER 2

2 Solid forms. Methods of preparation and investigations

The most used methods to obtain new solid forms are: recrystallization from solution (RC), "solvent drop" grinding (SDG), exposure to solvent vapor or vapor digestion (VDig) and slurring (SL) [Brittain 2009a].

Crystallization (RC): This is the most common methodology applied to derive new forms and for crystal growth. It is prepared a saturated solution of the compound with a solvent and allows evaporating the solvent.

Solvent drop grinding method (SDG): Solid samples were mixed manually in a mortar of agate while the solvent was added until it was obtained a dry composition.

Slurring procedure (SL): The solid material is suspended, usually for an extended period, in a quantity of solvent that is insufficient to dissolve it completely. Slurring experiments are usually carried out over periods of 2–4 weeks, or even longer.

Vapor digestion (VDig): Exposing the physical mixture of reactants to vapours of a solvent or mixtures of solvents for different periods of time.

In order to obtain single crystals of a substance, different methods were used such as: crystallization by slow evaporation of the liquid or solvent mixtures (RC), solid substance exposure at different humidity and temperature regimes, vapor diffusion (VDif), liquid diffusion or crystallization multilayer (LDif) [Stout *et al* 1989, Brittain 2009].

Vapor diffusion (VDif): Two vials are needed where one can fit inside the other: in the inner vial, the compound to be cristalized is dissolved in a small quantity of a moderately non volatile solvent; in the second vial a volatile solvent in which the compound is insoluble is added. The two solvents must be miscible.

Liquid-liquid difussion (Ldif): On this technique involves the use of two (or tree) solvents, one in which the material is soluble and a second in wich is insoluble. The first solvent is more volatile than the second.

CHAPTER 3

3 Experimental results

3.1 Ambazone monohydrate and anhydrous

Ambazone monohydrate $C_8H_{11}N_7S \cdot H_2O$ ([4-(2-(Diaminomethylidene)hydrazinyl) phenyl] iminothiourea) (AMB) is a compound with a relatively low solubility, has a molecular weight of 255.3 g/mol and melting point around at 192 °C and 194 °C, accompanied by decomposition [Fichtner *et al* 1983, Kuhnel *et al* 1988a]. Structural formula is shown in Figure 3.1.1.

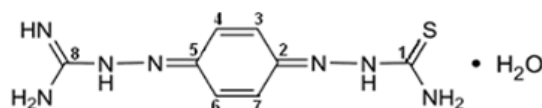


Figure 3.1.1. Structural formula of Ambazone

Ambazone anhydrous (AMBanh) was obtained by exposure of the ambazone monohydrate to heat treatment for 30 minutes at 140 °C, followed by slow cooling to 25 °C. Applying the methods described in Chapter 2 various samples were prepared which were subsequently investigated by analytical methods suitable for the study of solids, namely: thermal analysis (DTA-TGA), Powder X-ray Diffraction (PXRD) and X-ray Single-crystal diffraction, Fourier transformed infrared spectroscopy (FT-IR), Nuclear magnetic resonance (NMR) spectroscopy and Scanning electron microscopy (SEM). Table 3.1.1 provides information on sample preparation by different methods:

Table 3.1.1. Sample preparation

Precursors	Methods
AMBanh : Acetone	<i>Recrystallization (RC)</i> 2 days, 25 °C
AMB : H ₂ O	<i>Solvent drop grinding (SDG)</i> by manual grinding in agate mortar; 5 minute
AMB : AMBanh : Dichloromethane (10 mg : 70 mg : 2 ml) AMB : AMBanh : Dichl : H ₂ O (10 mg : 70 mg : 2 ml : 0.04 ml) AMBanh : Dichloromethane : H ₂ O (90 mg : 2 ml : 0.04 ml)	<i>Slurrying (SL)</i> 5 days

3.1.1 DTA-TGA analysis

Thermal measurements for AMB and AMBanh were carried out starting from room temperature up to 400 °C with a 10 °C/min heating rate. DTA-TG analyses for AMB (Figure 3.1.2.a) showed two well-defined thermal events: an endotherm signal at ~135°C associated with a TGA weight loss of ~6.5%, most likely corresponding to the water loss; an exotherm event at ~215°C associated with a TGA weight loss of 30.7% related to the thermal decomposition process. Due to the strong decomposition event, the melting of AMB is not clearly defined. In the case of AMBanh, only the exotherm decomposition is visible in the DTA trace and there is no visible endotherm related to water loss.

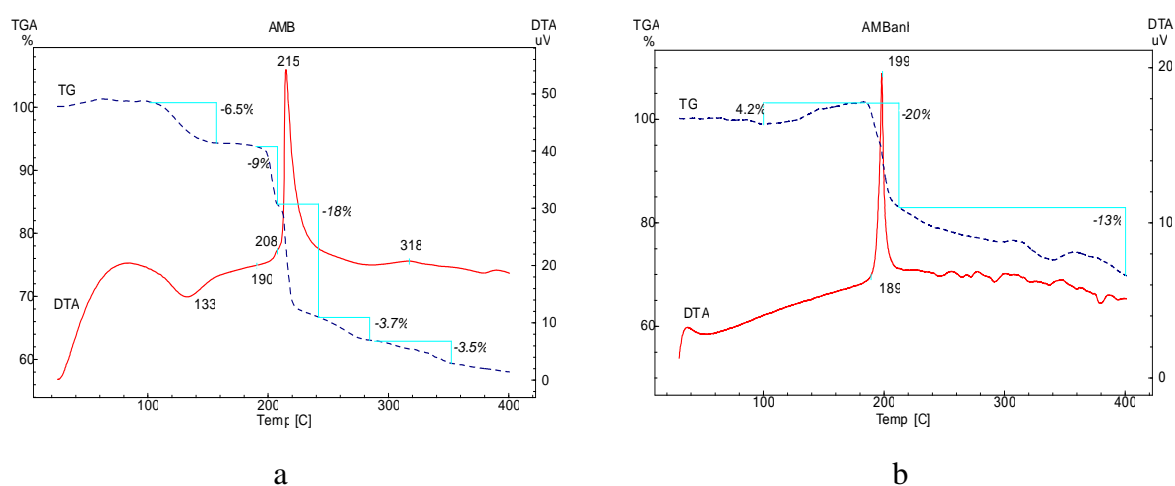


Figure 3.1.2. DTA-TGA thermograms for: AMB (a) and AMBanh (b).

3.1.2 Powder X-Ray Diffraction (PXRD)

PXRD analyses show that applying certain crystallization methods and certain solvents the ambazone monohydrate turn into the anhydrous form and vice versa. By crystallization of anhydrous ambazone with acetone is obtained an identical powder pattern of ambazone monohydrate and recrystallized with chloroform resulting anhydrous form (Figure 3.1.3.a). By applying the slurry method it was prepared a saturated solution of ambazone monohydrate and anhydrous with dichloromethane and another similar one also with dichloromethane but also with water (AMB : AMBanh : Dichl), (AMB : AMBanh : Dichl : H₂O), and were left in the slurry for 5 days (Figure 3.1.3.b). The X-ray powder diffraction analyze found that AMB + AMBanh + Dichl_SL is similar to AMBanh, but is different from sample prepared with water (AMB+AMBanh+Dichl+H₂O_SL), which is identical to ambazone monohydrate.

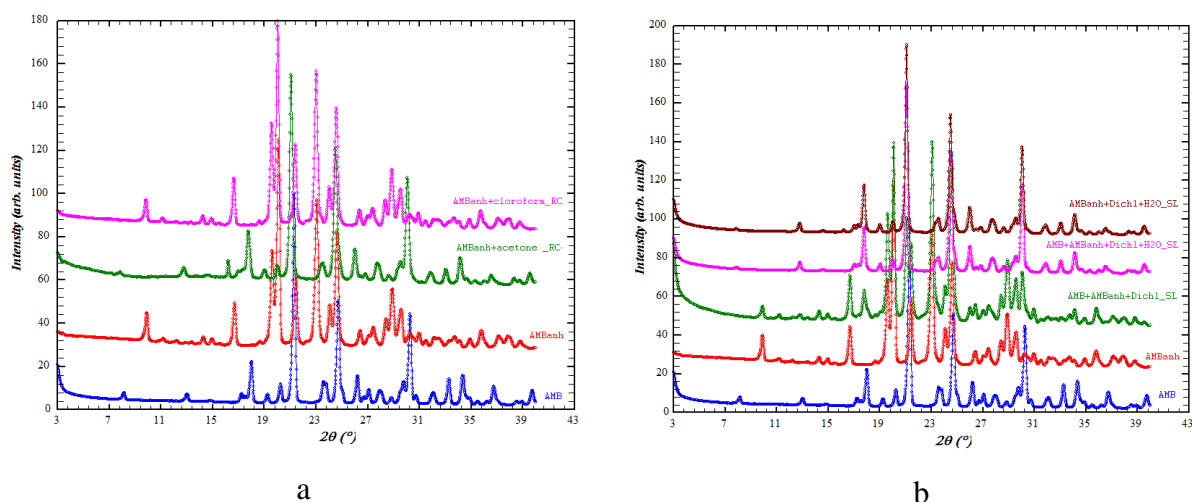


Figure 3.1.3. PXRD of forms obtained by crystallization from chloroform and acetone (RC) (a) and Slurry for 5 day (SL) (b) compared with AMB and AMBanh.

The structural changes that occur after recrystallization by different methods are shown in Figure 3.1.3.c. It is noted that according to the method of crystallization AMBanh becomes AMB and vice versa.

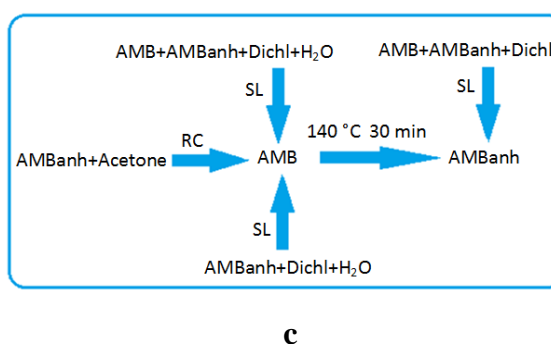


Figure 3.1.3. Transformation diagram due to the applied processes to the samples (c).

3.1.3 Variable Temperature Powder X-Ray Diffraction (VTPXRD)

Variable temperature PXRD was applied to ambazone monohydrate in order to follow any changes in the solid form by heating. An amount of AMB was heated to different temperatures in the temperature range of 90-210°C and PXRD was carried out at the respective temperatures (Figure 3.1.4.).

In the temperature range 25-90°C the PXRD patterns of AMB are similar and therefore there are no solid form changes taking place.

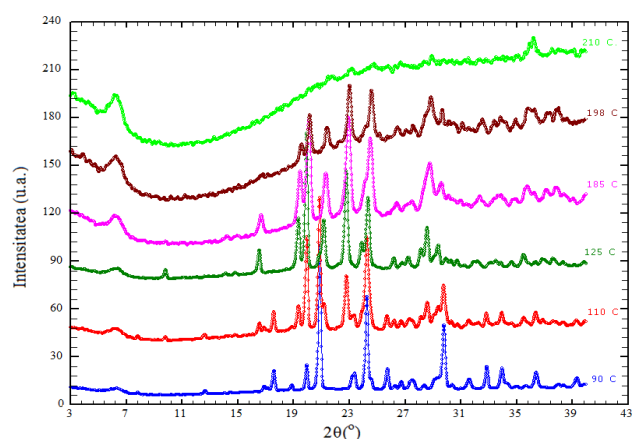


Figure 3.1.4. PXRD patterns obtained for form F1 heated in the temperature interval 90-210°C.

At 100°C, the anhydrous form of ambazone appears and maintains their crystallinity up to 198°C. From 210°C the material is completely amorphous. We can conclude that ambazone monohydrate is thermally stable in solid state up to 198°C, afterwards the structure collapses into amorphous phase.

3.1.4 Fourier Transformed Infrared Spectroscopy (FTIR)

FTIR spectra were recorded for ambazone monohydrate (AMB) and anhydrous form (AMBanh) and are presented in Figure 3.1.5. a,b. The FTIR analysis showed changes in the characteristic absorption bands of the primary and secondary amines. The two spectra are different due to changes in crystal structure by dehydration of ambazone.

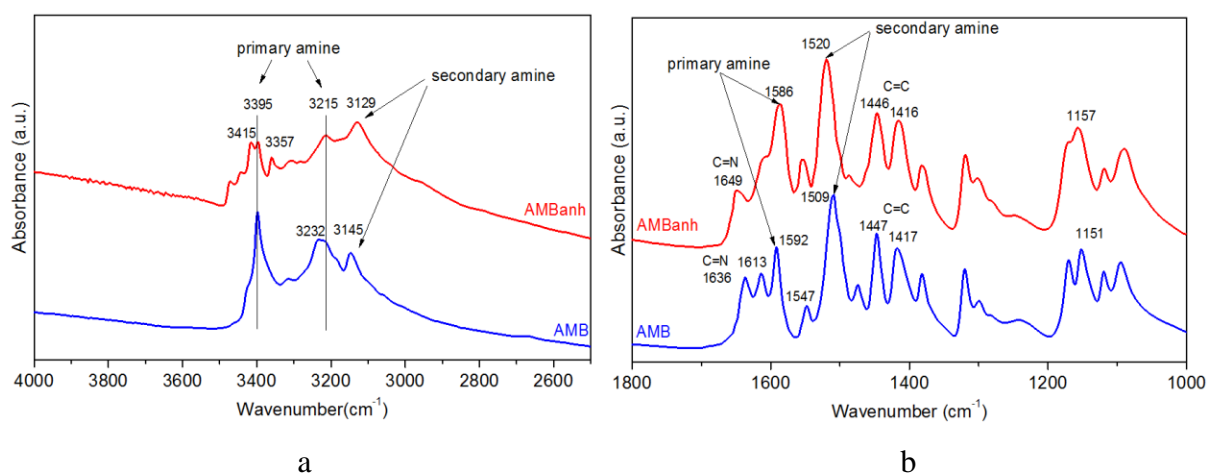


Figure 3.1.5. FTIR spectra obtained for ambazone monohydrate and anhydrous, in the range of 4000-2500 cm^{-1} (a) and 1800-1000 cm^{-1} (b).

For AMB were identified the stretching vibration of primary amines around ~ 3398 and 3232 cm^{-1} , respectively at ~ 3397 , 3415 and 3214 cm^{-1} for AMBanh (Figure 3.1.5.a). The stretching vibrations of secondary amine have been identified at $\sim 3145 \text{ cm}^{-1}$ for AMB, respectively $\sim 3129 \text{ cm}^{-1}$ for AMBanh [Socrates 2001]. For AMB, the medium intensity bands at 1636 and 1613 cm^{-1} (Figure 3.1.5.b) are attributable to $\text{C} = \text{N}$ deformation vibration [Stilinovic et al 2008], this vibration is identified around $\sim 1649 \text{ cm}^{-1}$ in the AMBanh spectra. The vibration from ~ 1592 , 1586 cm^{-1} for AMB respectively AMBanh is assigned to deformation of primary amine NH_2 [Socrates 2001]. The deformation vibration of secondary amine at $\sim 1509 \text{ cm}^{-1}$ corresponding to ambazone monohydrate is shifted to $\sim 1520 \text{ cm}^{-1}$ in the spectrum of anhydrous form (AMBanh).

3.1.5 Solid state CP/MAS NMR analysis

From ^{13}C CP/MAS NMR spectrum (Figure 3.1.6.), there were identified eight resonance lines corresponding to the eight carbon molecules found in the ambazone structure: (i) the resonance lines in the region 110-140 ppm are corresponding to non-equivalent protonation of carbons from the aromatic rings C3, C4, C6, C7, (ii) the two lines at ~ 146 ppm are attributed to non-protonation of the carbons from C2, C5, and (iii) resonance lines at 162 ppm and 175 ppm are assigned to C8 carbon and C1 carbon respectively.

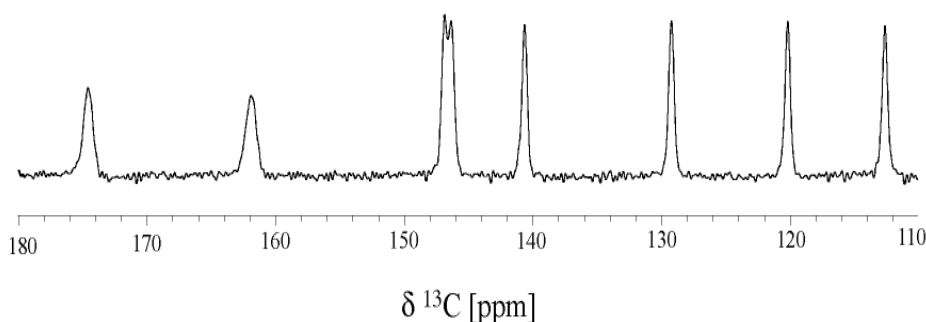


Figure 3.1.6. ^{13}C CP / MAS NMR spectrum of AMB ($\nu\text{R} = 15$ kHz, CP = 2 ms).

3.1.6 Scanning Electron Microscopy (SEM)

SEM images (Figure 3.1.7. a, b) present different morphology obtained for Ambazone monohydrate and anhydrous for.

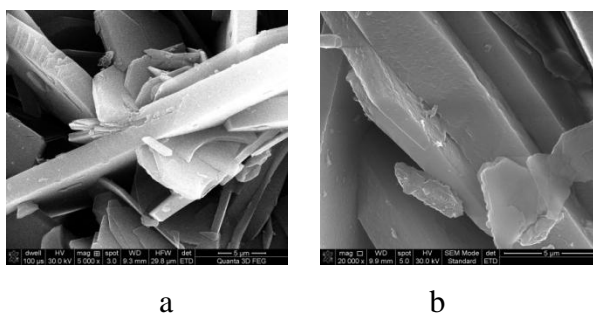


Figure 3.1.7. SEM images for AMB (a) and AMBanh (b).

3.1.7 Crystal and molecular structure determination from X-ray Single-crystal diffraction

Single crystals of ambazone monohydrate and ambazone anhydrous were obtained by applying multi-layer crystallization method. There were used three layers of liquid, superimposed over one another and allowed to diffuse.

AMB: From Ambazone monohydrate and acetone was obtained a saturated solution. This solution was placed in a tube and added pentane (2 ml) and ether (2 ml).

AMBanh: A saturated solution was obtained from Ambazone monohydrate with p-Aminobenzoic acid and nitromethane.

This solution was placed in a tube and tetrahydrofuran (2 ml) and hexane (2 ml) was added. The closed system was left to react for 5 days at room temperature. There were obtained plate-like crystals with suitable ~0.08 - 0.3 mm dimensions for single-crystal analysis (Figure 3.1.8. a, b).

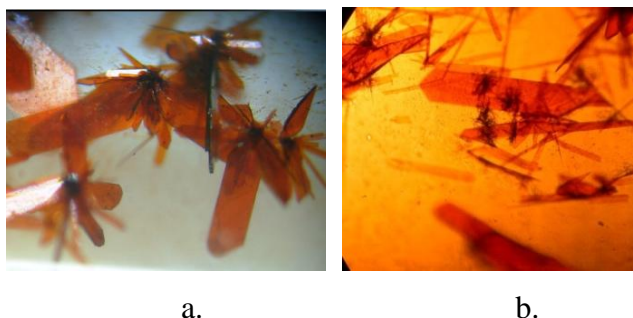


Figure 3.1.8. Single crystals for AMB (a) and AMBanh (b).

Single-crystal analysis led to the determination of the crystallographic system, cell parameters and the space group. Also, crystal structure determination revealed the molecular conformation, the hydrogen bonds and the molecular packing of the ambazone monohydrate molecules (Figure 3.1.9, 3.1.10.). There are four asymmetric units cell in the unit cell and one asymmetric unit contains one ambazone monohydrate molecule. The following hydrogen bonds are presented in the ambazone monohydrate structure: S1-N1: S1-N12: N14-O15 (water): O15-S1: N2-O15 (water). Water molecule link the two ambazone molecules by hydrogen bonds.

Crystallographic data for ambazone monohydrate

Molecular formula	C ₈ H ₁₁ N ₇ S H ₂ O
Molar mass	255.30 g/mol
Crystal system	monoclinic
Space group	P2 ₁ /c
Cell parameters	$a = 7.2008(10) \text{ \AA}$, $b = 7.2753(9) \text{ \AA}$, $c = 22.363(2) \text{ \AA}$ $\alpha = 90.00^\circ$, $\beta = 90.00^\circ$, $\gamma = 90.00^\circ$.
Cell volume	1171.55(20) Å ³
Z (No. molecules per unit cell)	4 (1 AMB molecule in the asymmetric unit)
Calculated density	1.368 g/cm ³
R factor	0.08
Goodness-of-fit on F ²	1.272.

Although all angles are 90 degrees, is a monoclinic crystallographic system.

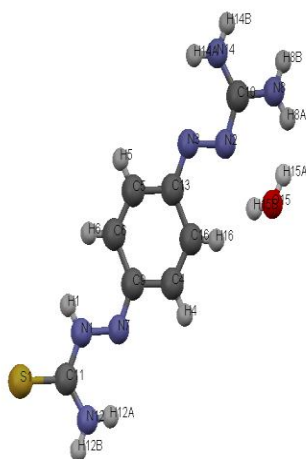


Figure 3.1.9. Molecular conformation of ambazone monohydrate

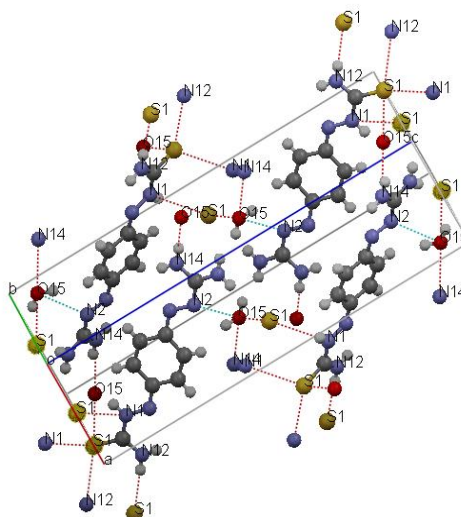


Figure 3.1.10. Molecular packing and H-bonding for ambazone monohydrate.

Single-crystal of Ambazone anhydrous analysis led also to the determination of the crystallographic system, cell parameters and the space group. Crystal structure determination revealed the molecular conformation, the hydrogen bonds and the molecular packing of the ambazone anhydrous molecules (Figure 3.1.11, 3.1.12.). There are two asymmetric units in the unit cell and two ambazone anhydrous molecules in the asymmetric unit. The following hydrogen bonds are present in the ambazone monohydrate structure: S1-N11, S1-N12, N6-N15). Ambazone molecules link together by hydrogen bonds.

Crystallographic data for ambazone anhydrous

Molecular formula	C ₈ H ₁₁ N ₇ S
Molar mass	237.30 g/mol
Crystal system	monoclinic
Space group	<i>P</i> 1 21 1 (no. 4)
Cell parameters	<i>a</i> = 7.847(10) Å, <i>b</i> = 17.856(2) Å, <i>c</i> = 8.365(2) Å $\alpha = 90.00^\circ$, $\beta = 109.45(2)^\circ$, $\gamma = 90.00^\circ$
Cell volume	1105.2(3) Å ³
Z (No. molecules per unit cell)	4, (1 AMBanh molecules in the asymmetric unit).
Calculated density	1.426 g/cm ³
R factor	0.0995
Goodness-of-fit on F ²	1.141

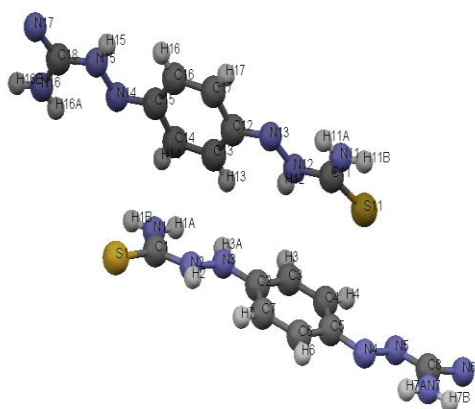


Figure 3.1.11. Molecular conformation of ambazone anhydrous.

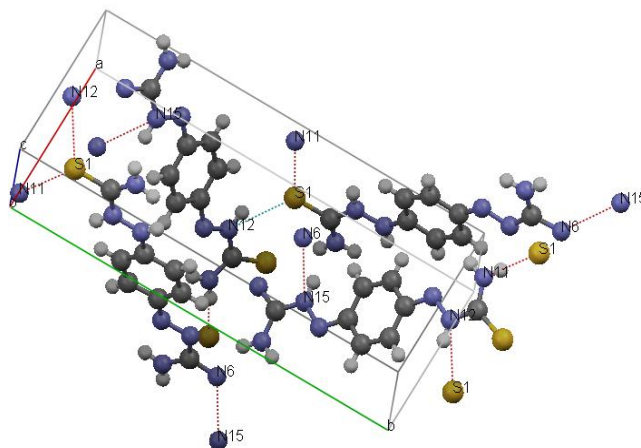


Figure 3.1.12. Molecular packing and H-bonding for ambazone anhydrous.

3.2 Ambazone with acetic acid

Ambazone monohydrate has $pK_a(B)$ values of: 6.27; 7.37; 10.67 [Kuhnel *et al* 1988], [Löber *et al* 1990, Petersen *et al* 1955] and acetic acid ($C_2H_4O_2$) has a $pK_a(A)$ value of about 4.76, reason for trying to obtain the salt of acetic acid with Ambazone. The samples were obtained by three methods: SDG, SL and VDig. All the resulting solids were characterized by PXRD (3.2.1) in order to identify the different solid forms. For each solid form additional analytical methods were applied for their further characterization (Sections 3.2.2 - 3.2.4).

3.2.1 Powder X-Ray Diffraction (PXRD)

The PXRD analysis led to the following results:

1. The PXRD patterns of the samples prepared by SDG method, using a 1:1 molar ratio between ambazone and acetic acid, were different from each other and from the PXRD pattern of the starting ambazone. These two different forms of ambazone with acetic acid were denoted with F1 (with molar ratio 1:1), respectively F2 (with molar ratio 2:1) (Figure 3.2.1).
2. The two samples obtained by the SL method, prepare in acetic acid alone or in mixture with dichloromethane had identical PXRD patterns with F2.
3. Four samples were prepared by VDig method by exposing ambazone monohydrate powder to acetic acid vapors for different period of times. The PXRD analysis showed that the sample exposed to vapors for 32 h is a new solid form, denoted F3. The samples exposed to acetic acid vapors for 14 and 30 days had identical PXRD patterns with F2. The sample

obtained after 5 days exposure showed a mixture of the forms F2 and F3 (Figure 3.2.2.). One can conclude that after 32 h vapor exposure, the first new F3 form develops, followed by its partial transformation to F2 after 5 days and its complete transformation to F2 after 14 days. Form F2 remains stable even after vapor exposure of 30 days.

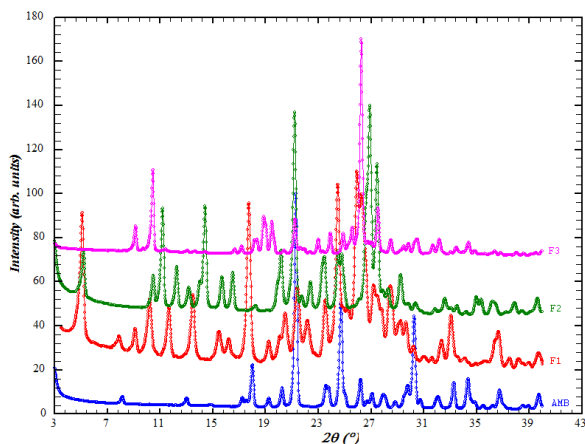


Figure 3.2.1. PXRD patterns for the solid forms of ambazone with acetic acid compared with the PXRD pattern of ambazone monohydrate.

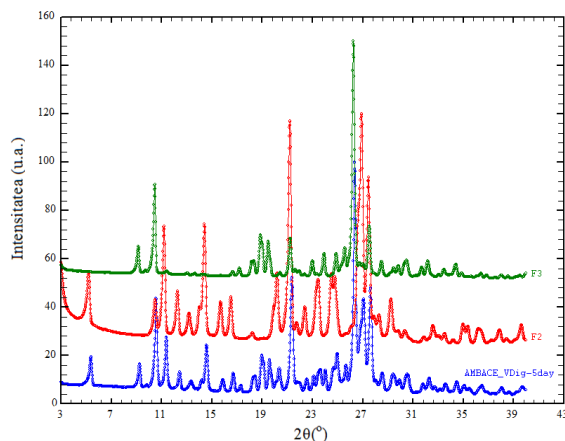


Figure 3.2.2. PXRD patterns obtained for AMBACE_VDig-5Day and F2, F3 samples.

The PXRD patterns of the forms F2 and F3 were indexed and the results are as follows:

- form F2 crystallizes in the monoclinic C_2 space group with the following cell parameters: $a = 16.548 \text{ \AA}$, $b = 7.1592 \text{ \AA}$, $c = 16.5713 \text{ \AA}$, $\beta = 96.521^\circ$, $\alpha = \gamma = 90^\circ$.
- Form F3 crystallizes in the monoclinic $C_{2/c}$ space group with the following cell parameters: $a = 19.0198 \text{ \AA}$, $b = 9.2478 \text{ \AA}$, $c = 17.8843 \text{ \AA}$, $\beta = 92.535^\circ$, $\alpha = \gamma = 90^\circ$.

3.2.2 DTA-TGA analysis

The thermograms obtained for the solid forms F1, F2 and F3 are shown in Figure 3.2.3.b-d. The thermogram of ambazone monohydrate is included for comparison (Figure 3.2.3. a). Thermogravimetric analysis of form F1 (Figure 3.2.3.b.) shows that it is thermally stable up to 60°C given the fact that no weight loss is detected in the TGA trace. In the temperature interval $60\text{--}158^\circ\text{C}$ the DTA curve shows an endothermic event with a maximum at 115°C , while the TGA trace shows a weight loss of $\sim 15\%$. This event is most likely related to dehydration and the loss of acetic acid taking place together with the melting of the form. A second exothermic event was observed in the temperature interval $158\text{--}205^\circ\text{C}$, with a maximum located at about 172°C , which is associated with a weight loss of 10% in the TGA.

This event is likely related to sample thermal decomposition, given the fact that additional weight losses of 7.5% and 11% are observed in the temperature interval of 205–400°C.

DTA-TGA analysis of form F2 (Figure 3.2.3.c.) shows three, well-defined thermal events. The first event is endothermic, located at about 65°C and has an associated TGA weight loss of 2% related to the loss of water. The second event, also endothermic, located at 130°C is associated with a TGA weight loss of 25% and is most likely related to the loss of acetic acid and melting of the form. One should remark that in form F1 these two events are overlapping. Further, a third exothermic event is observed and is associated with thermal decomposition of the form.

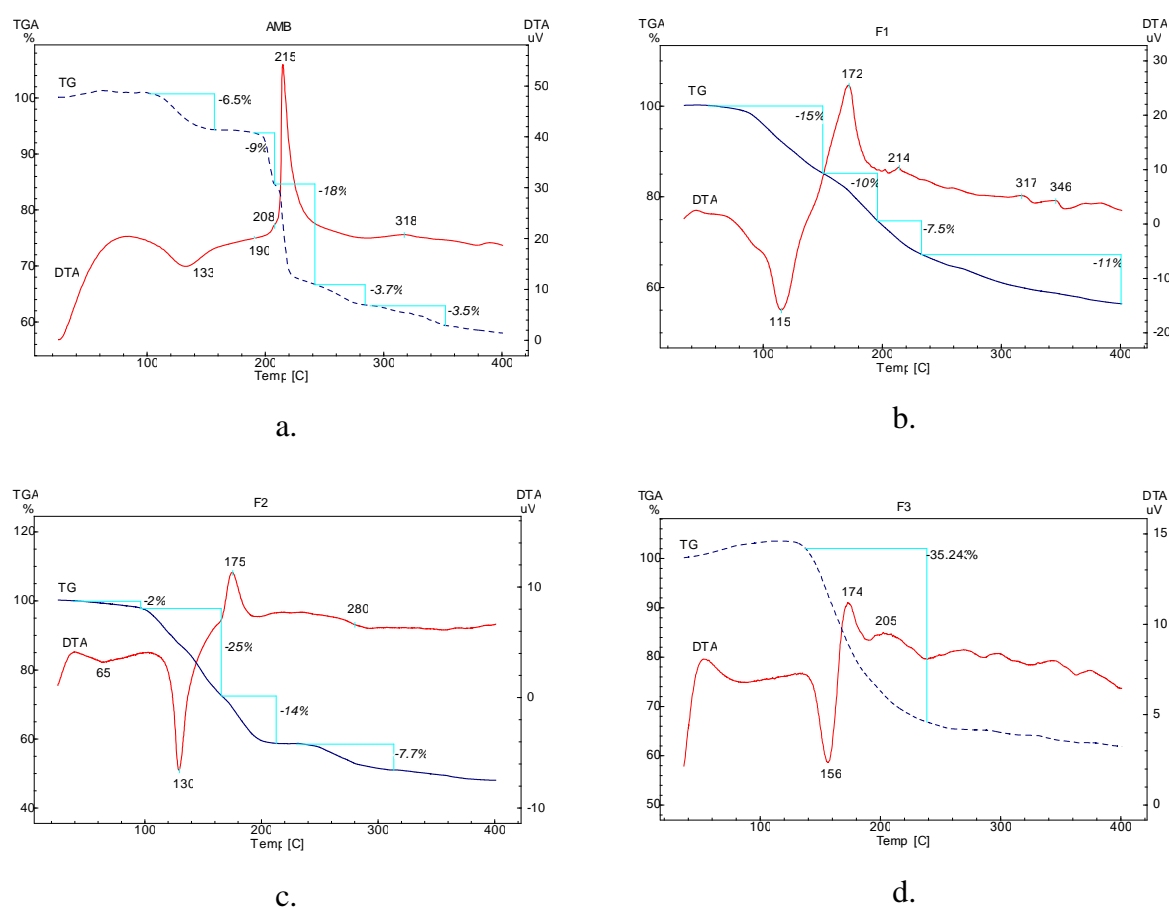


Figure 3.2.3. DTA-TGA thermograms of: AMB (a), F1(b), F2 (c) and F3 (d) forms

Thermal analysis of form F3 (Figure 3.2.3.d.) shows two major events. A first endothermic event present at 156°C corresponds to the loss of acetic acid (indicated by the TGA weight loss) and melting of the form. The second exothermic event and the corresponding weight loss are related to the thermal decomposition process, as in the case of forms F1 and F2.

3.2.3 Variable temperature powder X-ray diffraction

Variable temperature PXRD was applied to form F1 in order to follow any changes in the solid form by heating. A sample of form F1 was heated to different temperatures in the temperature interval 25-110°C and PXRD was carried out at the respective temperatures (Figure 3.2.4.).

In the temperature interval 25-82°C the PXRD patterns are similar and therefore there are no solid form changes. At 100°C, the amorphous form appears together with F1, while at 110°C, the material is completely amorphous. We can conclude that form F1 is relatively thermally stable in solid state up to 100°C, after which the structure collapses into amorphous phase.

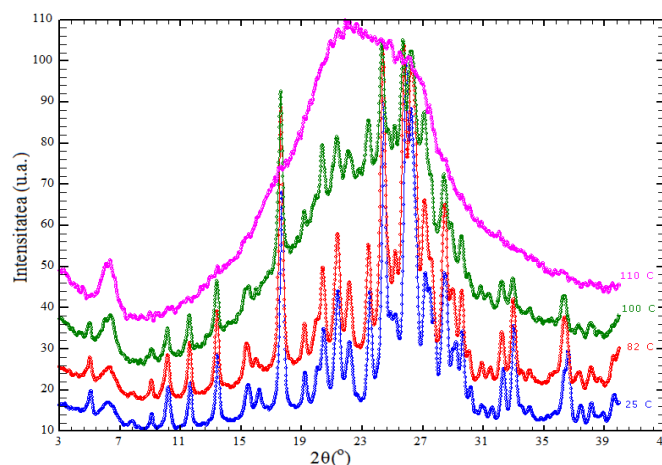


Figure 3.2.4. PXRD patterns obtained for F1 form heated in the 25-110°C interval temperature.

3.2.4 Fourier Transformed Infrared Spectroscopy

FTIR spectra were recorded for ambazone monohydrate AMB and new solid forms F1, F2 and F3 (Figura 3.2.5. a,b). The FTIR analysis showed changes in the characteristic absorption bands of the primary and secondary amines. These changes can be explained by the protonation of the ambazone amino groups (Table 3.2.1.).

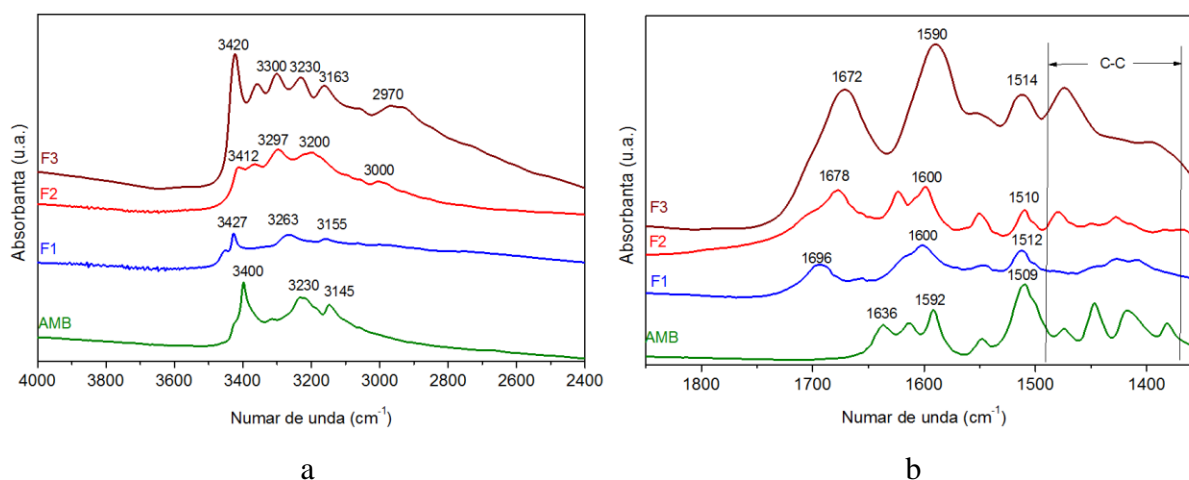


Figure 3.2.5. FTIR spectra of spectral range 4000-2400 cm^{-1} (a) respectively 1850-1300 cm^{-1} (b) for AMB, F1, F2 and F3.

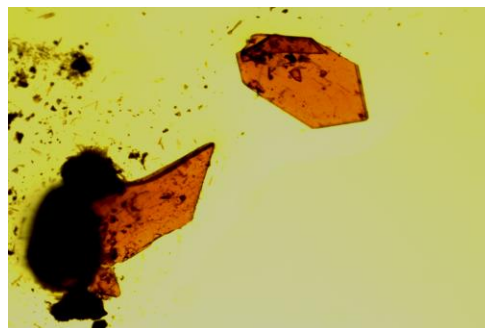
Table 3.2.1. FTIR analysis for AMB, F1, F2 and F3 forms.

AMB	~3400, 3230 cm ⁻¹ NH ₂	~3145cm ⁻¹ NH ~ 1592, 1509 cm ⁻¹	~1636 cm ⁻¹ C=N	C-C ~1447, 1417 cm ⁻¹
F1	~3427,3263 cm ⁻¹ NH ₃ ⁺	~3155 NH ₂ ⁺ ~1512, 1600 cm ⁻¹	~1696 cm ⁻¹ C=N	C-C ~1429, 1408 cm ⁻¹
F2	~3412, 3297 NH ₃ ⁺	~3200 NH ₂ ⁺ ~1510, 1600 cm ⁻¹ New vibration at 3000 cm ⁻¹	~1678 cm ⁻¹ C=N	C-C ~1480, 1427 cm ⁻¹
F3	~3420, 3300 NH ₃ ⁺	~3163 NH ₂ ⁺ ~1514, 1590 cm ⁻¹ , New vibration at 3230 and 2970 cm ⁻¹	~1672 cm ⁻¹ C=N	C-C ~1476, 1396 cm ⁻¹

3.2.5 Crystal and molecular structure determination from X-ray Single-crystal diffraction

Single crystals of ambazone with acetic acid were obtained by applying the vapor diffusion method. A saturated solution of ambazone with acetic acid and dichloromethane was exposed to diethyl ether vapors for 5 days. This resulted in plate-like crystals (Figure 3.2.6.) with 0.08 - 0.3 mm, suitable dimensions for single-crystal analysis.

Single-crystal analysis led to the determination of the crystallographic system, cell parameters and the space group. Also, crystal structure determination revealed the molecular conformation, the hydrogen bonds and the molecular packing of the ambazone acetate molecules (Figure 3.2.7., 3.2.8.).

**Figure 3.2.6.** Single crystal of ambazone acetate.

Crystallographic data for ambazone acetate

Molecular formula	C ₁₂ H ₁₈ N ₇ O ₄ S
Molar mass	356.39 g/mol
Crystal system	monoclinic
Space group	C 2/c (no. 15)
Cell parameters	$a = 19.1681(16) \text{ \AA}$, $b = 9.3693(17) \text{ \AA}$, $c = 17.976(3) \text{ \AA}$ $\alpha = 90.00^\circ$, $\beta = 94.00(1)^\circ$, $\gamma = 90.00^\circ$ $3220.48(80) \text{ \AA}^3$
Cell volume	8 (1 molecule of ambazone and 2 acetic acid molecules in
Z (No. molecules per unit cell)	the asymmetric unit).
Calculated density	1.470 g/cm^3

R factor	0.0877
Goodness-of-fit on F ²	1.272

There are eight asymmetric units in the unit cell and one asymmetric unit contains one ambazone and two acetate molecules. The following hydrogen bonds are present in the ambazone acetate structure: N6-O1, N5-O2, N5-O3, N4-S1, N1-O2, O4-O1.

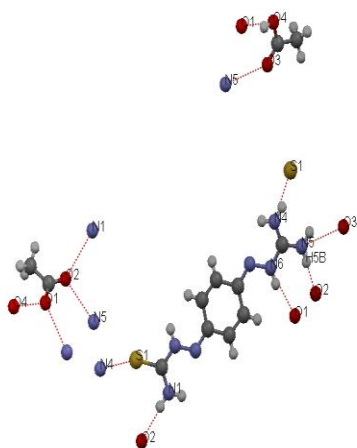


Figure 3.2.7. Molecular conformation and H-bonding of ambazone acetate.

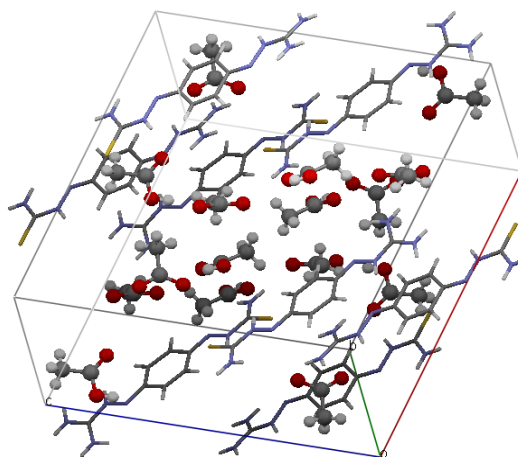


Figure 3.2.8. Molecular packing for ambazone acetate.

3.3 Ambazone with hydrochloric acid

By SDG method has been prepared a sample of AMB with HCl, in molar rate 1:1, for 4 hours, at room temperature. The Ambazone hydrochloride (AMBHCl_SDG) was prepared by grinding of 255.3 mg AMB with 2 mL HCl aqueous solution (0.5 M) in an agate mortar at room temperature, until a dried compound was obtain. It was observed the change of AMB colour from reddish-brown to yellowish-brown.

3.3.1 DTA-TGA analysis

The DSC curves obtained for pure AMB and for the compound obtained by SDG method (AMBHCl_SDG) are different (Figure 3.3.1). The curve for the pure AMB revealed a broad endothermic signal from 105 to 143°C, with a maximum at 125°C and $\Delta H = 36$ kJ/mol, that corresponds to the loss of the water molecule followed by sharp exothermic signal at 204°C, $\Delta H = 75$ kJ/mol due to the melting with decomposition of AMB.

The DSC curve for AMBHCl_SDG shows three signals: a broad endothermic signal with maximum at 77°C, $\Delta H = 38$ kJ / mol, assigned to loss of water molecules, which appears

in the DSC curve for AMB at about 125°C, the second broad endothermic signal located between 121-160°C, with maximum at 144°C, and $\Delta H = 18 \text{ kJ/mol}$, most likely due to loss of HCl and that is not found in the DSC curve for AMB.

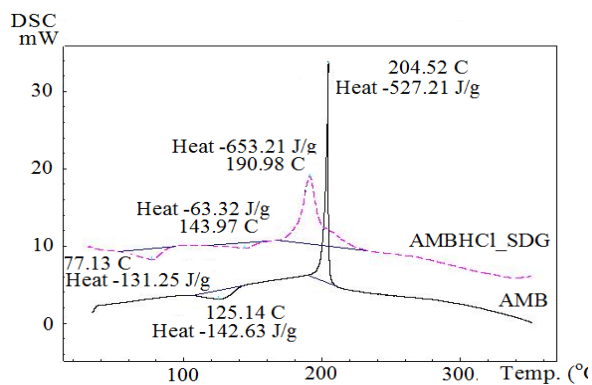


Figure 3.3.1. DSC analysis for AMB and AMBHCl_SDG.

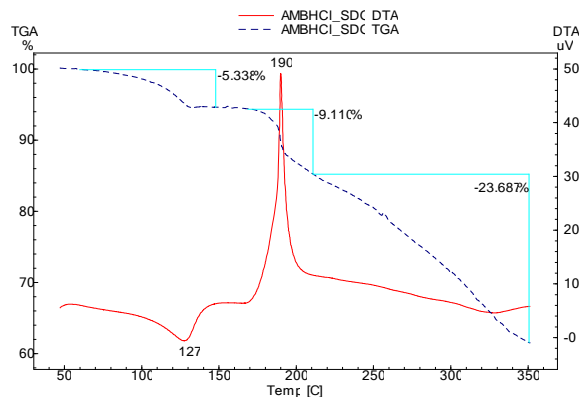


Figure 3.3.2. DTA-TGA traces for AMBHCl_SDG.

The third signal is the exothermic one which has a maximum at 190°C with $\Delta H = 185 \text{ kJ/mol}$, corresponding to the melting with decomposition of the sample. For AMB, this exothermic signal occurs at 204°C. From simultaneous DTA-TGA measurements made for AMBHCl_SDG (Figure 3.3.2.) it appears that mass loss occurs due to elimination of water and hydrochloric acid. These mass losses correspond to phenomena that have been identified in DSC measurements.

3.3.2 Powder X-ray diffraction

From Powder X-ray Diffraction of AMB and AMBHCl_SDG (Figure 3.3.3.) one can observe a significant difference between the two powder diffraction patterns.

The PXRD patterns of the AMBHCl_SDG were indexed [Boultif *et al* 2004] and the results are: crystallizes in a monoclinic system with the following lattice parameters: $a = 7.006 \text{ \AA}$, $b = 13.017 \text{ \AA}$, $c = 16.959 \text{ \AA}$, $\beta = 107.17^\circ$ and unit cell volume $V = 1477 \text{ \AA}^3$. The most likely space group is $P_{21/c}$.

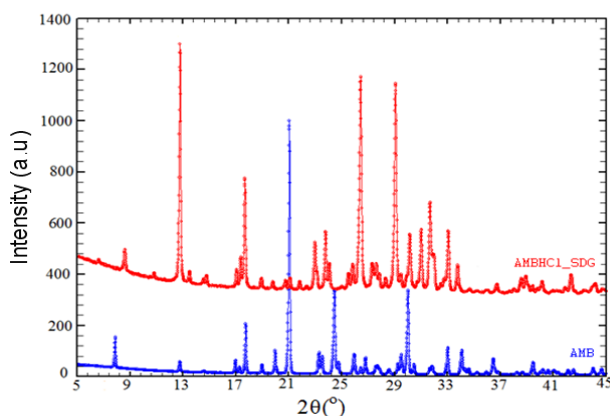


Figure 3.3.3. X-ray Powder Diffraction patterns for AMB and AMBHCl_SDG.

3.3.3 Fourier Transformed Infrared Spectroscopy

In the FTIR spectra obtained for (AMBHCl_SDG) is observed a shift to higher values compared to AMB spectrum. These is due to secondary protonated amines (signal at ~ 2980 cm^{-1}) and respectively at the primary amine (~ 1686 cm^{-1}). Salt formation is motivated by the appearance of a band at ~ 3267 cm^{-1} (Figure 3.3.4.a.; Figure 3.3.4.a.) [Socrates 2001].

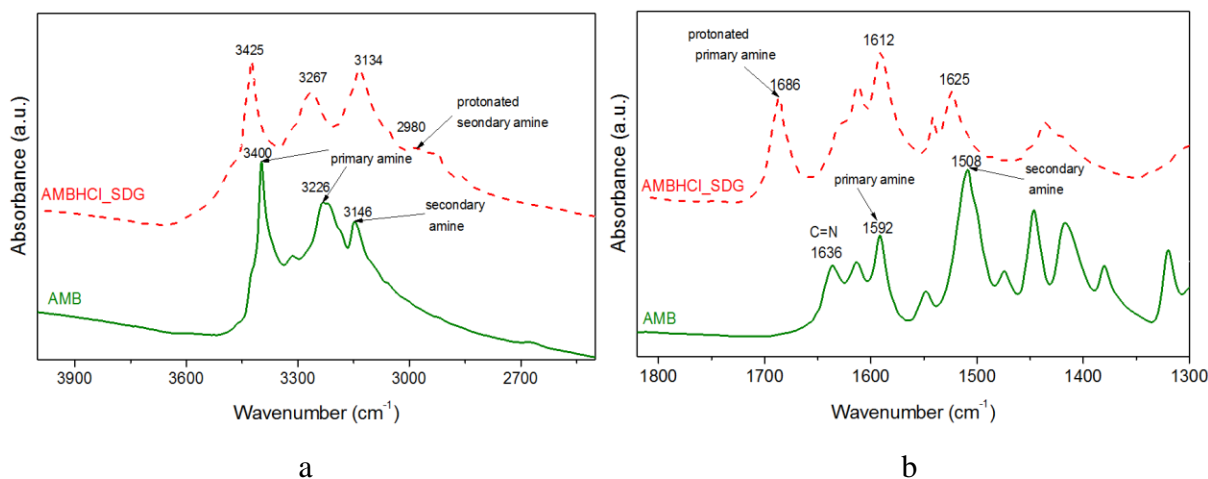


Figure 3.3.4. FTIR for AMB and AMBHCl_SDG in the 4000–2500 cm^{-1} (a) and 1800–1300 cm^{-1} (b) spectral range.

3.3.4 Solid state ^{13}C and ^{15}N NMR analysis

The ^{13}C CP/MAS spectra of the AMB and AMBHCl_SDG are shown in Figure 3.3.5.a. Both spectra consist of eight resonance lines, corresponding to the eight carbon sites in the molecular structure of the studied compounds. The main feature of these ^{13}C CP/MAS spectra is the important shift of the resonance lines of AMBHCl_SDG compound compared with the similar spectrum which correspond to pure AMB. Most probably this line shift can be attributed to the aromatic ring current effect, [Gomes *et* Mallion 2001] and the presence of Cl were disrupts a possible p–p stacking in AMB. Since all the AMB and AMBHCl_SDG resonance lines are not multiplied, we can draw the conclusion that there is only one molecule per asymmetric unit of both.

The ^{15}N CP/MAS spectrum (Figure 3.3.5.b) consists of seven resonance lines, according to the molecular structure of AMBHCl_SDG. These lines are assigned as follows: two NH_2 groups with resonances at 44.3 and 45.8 ppm; a NH_2^+ group with the resonance line at 105.6 ppm; two NH groups at 141 and 171.5 ppm, respectively, and two non-protonated nitrogens linked to the aromatic ring, which exhibit resonances at 266 and 282.8 ppm. ^{13}C and ^{15}N NMR data which establishes that asymmetric unit contains one molecule.

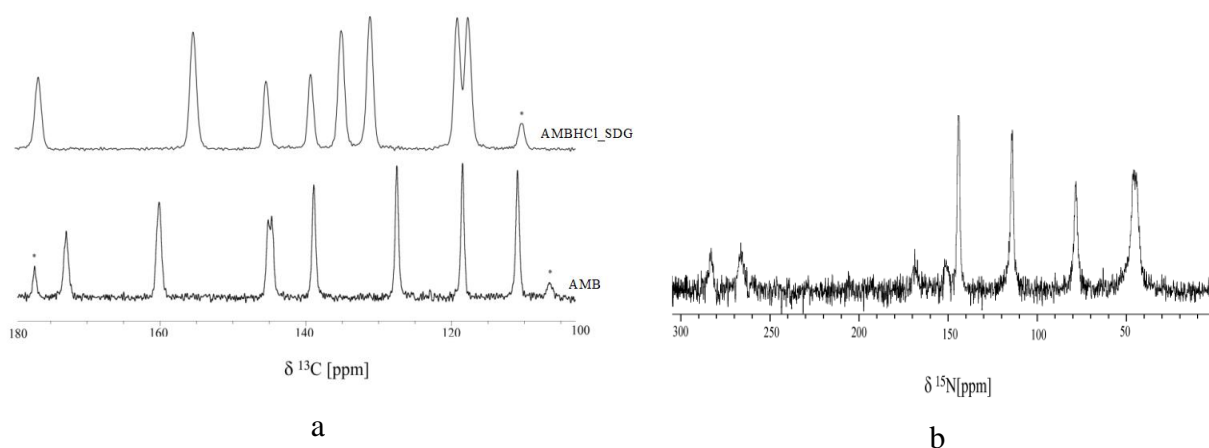


Figure 3.3.5. The ^{13}C CP/MAS NMR spectra of AMB and AMBHCl_SDG, recorded at spinning frequency $mR = 10$ kHz with a $CP = 1,5$ ms (a). The asterisks indicate spinning sidebands. The ^{15}N CP/MAS RMN for AMBHCl_SDG (b).

3.4. Ambazone with glutamic acid

L-Glutamic Acid ($\text{C}_5\text{H}_9\text{NO}_4$) (Glu), is a non-essential amino acid and has applications in cancer therapy [Otsuka *et al* 1994]. Ambazone (AMB), contains several amino groups and hence their property to capture electrons and thus the formation of salts with various acids. Glutamic acid has $pK_a = 2.01$ for COOH value and pK_a of ambazone: 6.27, 7.37, 10.67, indicating the possibility of obtaining the combination of salts.

Solvent-drop grinding experiments were performed by placing 255.3 mg AMB with 147.13 mg Glu by addition of water in an agate mortar at room temperature, until a dried compound was obtained. There was a change in color of mixing.

3.4.1. DSC, DTA-TGA analyses

DSC traces obtained for AMB and AMBGlu_SDG compounds (Figure 3.4.1.a) evidenced water loss by the appearance of an endothermic signal at 125°C for AMB and 97°C for the compound AMBGlu_SDG and $\Delta H = 19$ kJ / mol.

The exothermic sharp signal at 204.5°C , $\Delta H = 75$ kJ/mol for AMB is moved in the case of the prepared compound by SDG at 187.8°C , $\Delta H = 106$ kJ/mol, proof of decomposition overlapped with melting.

DTA-TGA thermograms for AMB and AMBGlu_Glu (Figure 3.4.1.b) showed differences. Thermograms for AMBGlu_Glu showed three well-defined thermal events: an endotherm event at $\sim 107^\circ\text{C}$ associated with a TGA weight loss of $\sim 5.84\%$, most likely corresponding to the water loss; the second endotherm event at $\sim 192^\circ\text{C}$, associated with a

TGA weight loss of 7,46%, $T_{\text{onset}} = 189^{\circ}\text{C}$ corresponding to the glutamic acid loss and beginning of melting process of AMBGlu_SDG compound; an exotherm event at $\sim 204^{\circ}\text{C}$ associated with a TGA weight loss of 9% related to the thermal decomposition process.

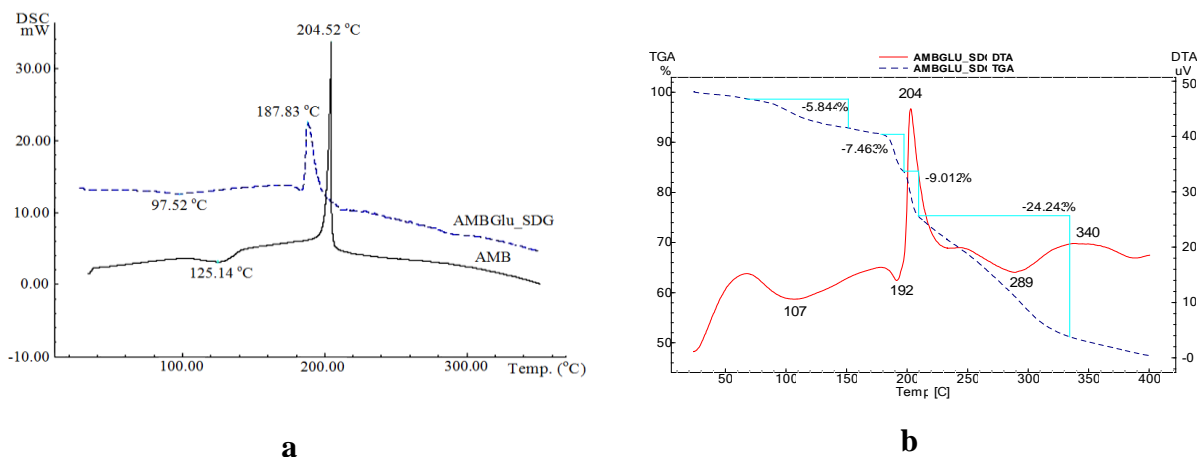


Figure 3.4.1. DSC traces for AMB and AMBGlu_SDG (a), DTA-TGA thermograms for AMBGlu_SDG (b).

Therefore AMBGlu_SDG thermal behavior is totally different from AMB and indicate the glutamate salt formation .

3.4.2. Powder X-Ray Diffraction

Powder diffraction pattern for AMBGlu_SDG (Figure 3.4.2.) is totally different from patterns of AMB and Glu, therefore a new solid form was obtained. By indexed procedure it was established that crystallize in monoclinic system space group probably $P2_1$. It has the following lattice parameters: $a = 9.8352 \text{ \AA}$, $b = 4.7014 \text{ \AA}$, $c = 40.0987 \text{ \AA}$, $\beta = 94.5050^\circ$, $V = 1844 \text{ \AA}^3$.

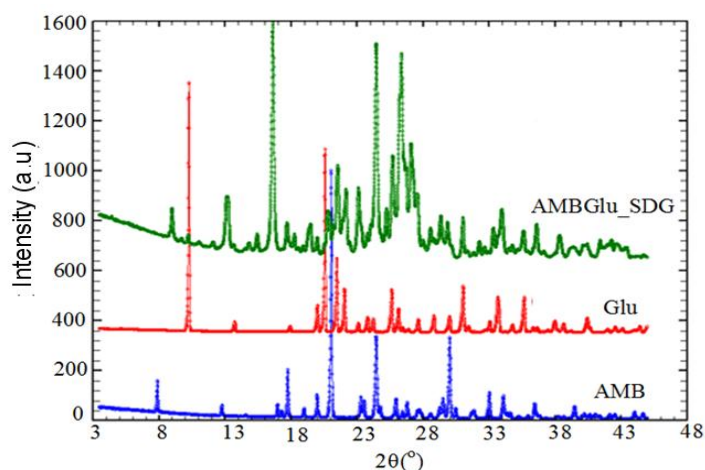


Figure 3.4.2. PXRD for AMB, Glu and AMBGlu_SDG.

3.4.3. Fourier Transformed Infrared Spectroscopy

FTIR spectra obtained for AMB, Glu and AMBGlu_SDG are shown in Figure 3.4.3 a,b. For the new obtained compound AMBGlu_SDG the vibrations at $\sim 3426 \text{ cm}^{-1}$ are

assigned to the primary amino group. The vibrations at $\sim 3258\text{ cm}^{-1}$ correspond to the protonated primary amino group NH_3^+ . The band located at 3145 cm^{-1} in AMB is shifted to $\sim 3158\text{ cm}^{-1}$ in the AMBGlu_SDG spectrum; it confirms the secondary amine protonation [Ivanova *et al* 2010].

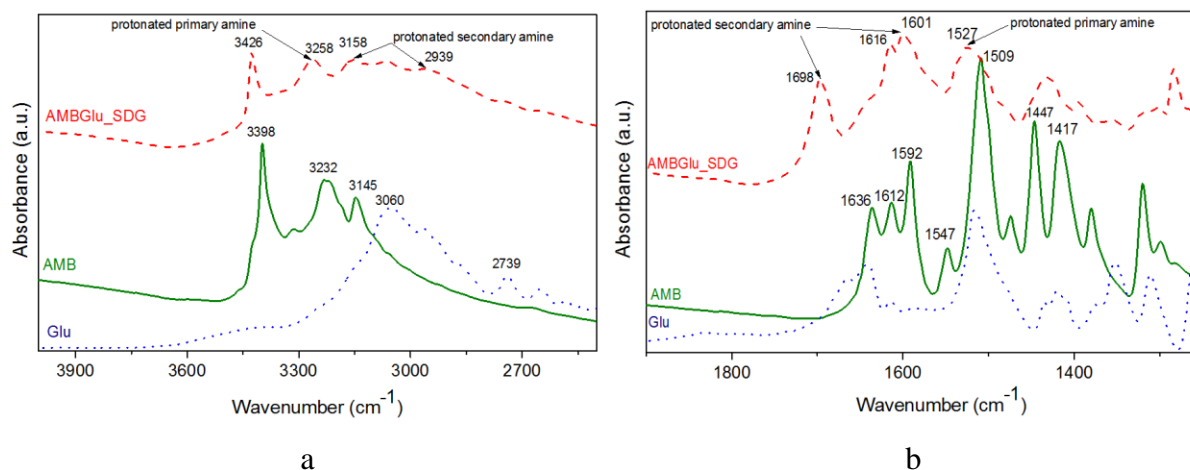


Figure 3.4.3. FTIR spectra of AMB, AMBGlu_SDG and Glu in $4000\text{-}2500\text{ cm}^{-1}$ (a) and $1800\text{-}1000\text{ cm}^{-1}$ (b) spectral domain.

The band located at $\sim 2930\text{ cm}^{-1}$ can be attributed to the NH_2^+ stretching vibration. The broad band at 1698 cm^{-1} (medium intensity) can correspond to the NH_2^+ deformation vibration in the solid form. The secondary amine presents a band of medium intensity at 1616 cm^{-1} deformation vibration of the protonated secondary amine NH_2^+ . In the $1650\text{-}1475\text{ cm}^{-1}$ spectral range, the IR bands at 1601 and 1527 cm^{-1} can be assigned to the NH_3^+ , δas^+ and δas^- bending vibrations [Ivanova *et al* 2010]. Based on the vibrational frequency's shifts and the new recorded bands one can conclude that a new solid form of ambazone was formed, i.e. an ambazone–glutamate salt.

3.4.4. ^{13}C solid state NMR analysis.

The ^{13}C CP/MAS spectra of the AMB, Glu, and AMBGlu_SDG are shown in the Figure 3.4.4. The NMR spectra of AMB and Glu consist of eight, respectively five resonance lines, corresponding to the carbon sites in the molecular structure of these two compounds. The chemical shifts of the resonance lines are illustrated in Table 3.4.1. Regarding the Glu molecule, a full assignment was possible taking as a reference the ^{13}C liquid-state NMR spectrum. Analyzing the resonance lines, one can conclude that (i) there are two conformationally non-equivalent Glu molecules in the asymmetric unit of the AMBGlu_SDG solid form and (ii) the line at 180.1 ppm (and 181.0 ppm , respectively) indicates the presence of COO^- site, which proves that AMBGlu_SDG belongs to the salts class. The presence of a

small quantity of Glu which remains after the chemical reaction with AMB is indicated by black arrows in Figure 3.4.4. [SDBS 2007].

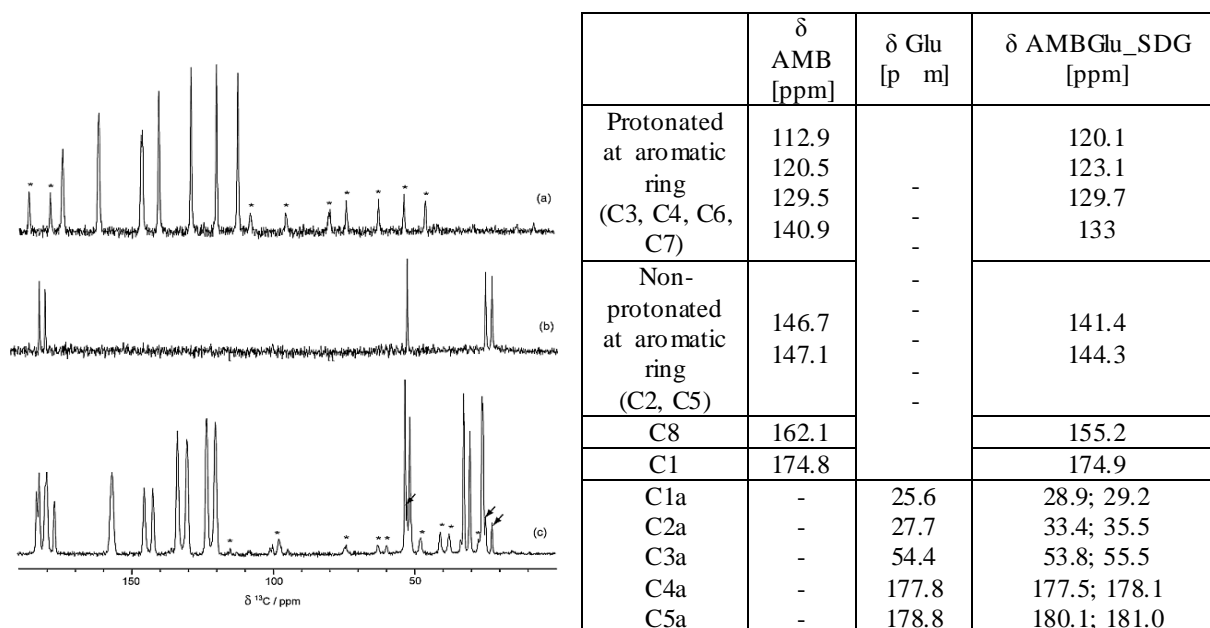


Figure 3.4.4. ^{13}C CP/MAS NMR spectra of AMB (a), Glu (b), and AMBGlu_SDG (c).

Table 3.4.1. Chemical shift ^{13}C CP/MAS NMR for AMB, Glu and AMBGlu_SDG.

3.5. Ambazone with p-Aminobenzoic acid

p-Aminobenzoic acid (PABA) or vitamin B₁₀ it's a organic compound with chemical formula ($\text{NH}_2\text{O}_2\text{C}_7\text{H}_7$), poorly soluble in water, with molecular mass of 137.14 g/mol and melting point 187°C, it is nontoxic, being used in treating cancer melanoma and in the antitumor activity of ionizing radiation [Chakrapani *et al* 2008]. Because both ambazone and p-Aminobenzoic acid have positive effects in antitumor treatments, it was tried to obtain a new form by combining their solids. The modalities of obtaining new forms occurred starting from the ambazone with para-aminobenzoic acid, in 1:1 stoichiometry, mixing in an agate mortar with water (SDG method), at constant temperature, for 30 minute.

3.5.1. DSC, DTA-TGA analysis

DSC curve shows two signals for AMBPABA_SDG compound (Figure 3.5.1.): an endothermic peak between 80 and 100°C, corresponding to loss of water molecules and a broad exothermic peak between 165 and 195°C, probably due to overlapping melting with decomposition. DTA-TGA thermograms obtained for AMBPABA_SDG compound (Figure 3.5.2.), indicates by presence of PABA, remove from lower temperature the water loss, than the temperature recorded for pure compound AMB, an event highlighted by two mass losses

of 5.6 and 4.2% respectively, the to two signals corresponding to broad endothermic peaks at 62°C and 92°C (Figure 3.5.2.). Melting and decomposition occurs between 140 and 185°C with a mass loss of 7.8%, which corresponds to a broad exothermic peak temperature in the range of 100-186°C, with maximum at 176°C. The final mass loss of 23.5% occurs in the range 190-300°C corresponding to the elimination of volatile components which results by decomposition of compound AMBPABA_SDG.

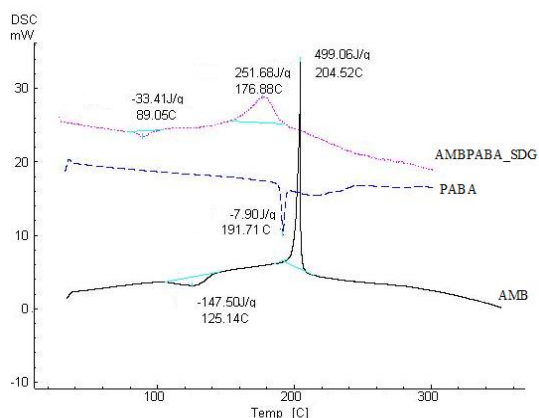


Figure 3.5.1. DSC curves of AMB, PABA and AMBPABA_SDG

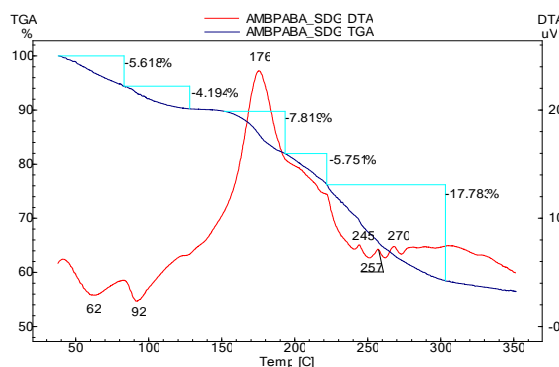


Figure 3.5.2. DTA-TG thermograms for AMBPABA_SDG.

3.5.2. Powder X-Ray Diffraction (PXRD)

The PXRD pattern for AMBPABA_SDG is different from AMB and PABA, which confirms the obtained new solid form. By indexing procedure the lattice parameters of the unit cell were determined: $a = 14.294 \text{ \AA}$, $b = 9.162 \text{ \AA}$, $c = 8.777 \text{ \AA}$, $\alpha = 95.90^\circ$, $\beta = 100.63^\circ$, $\gamma = 91.73.15^\circ$.

The compound AMBPABA_SDG crystallizes in the triclinic system (Figure 3.5.3.).

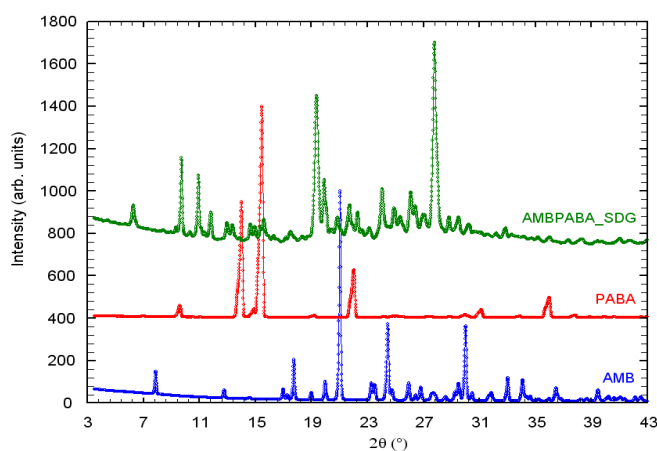


Figure 3.5.3. Powder X-ray Diffraction patterns of AMB, PABA and AMBPABA_SDG.

3.5.3. Fourier Transformed Infrared Spectroscopy

From the analysis of spectral absorption bands obtained for AMB and AMBPABA_SDG (Figure 3.5.4.) there were evidenced stretching vibrations of primary amino group NH_2 which appear modified in the spectrum of the new compound obtained by SDG method. FTIR measurements revealed modified NH stretching absorption bands of

amines [Otsuka et al 2010], due to the protonation of the primary amine and secondary amine, which demonstrates the formation of ambazone p-aminobenzoate salt (Table 3.5.1.).

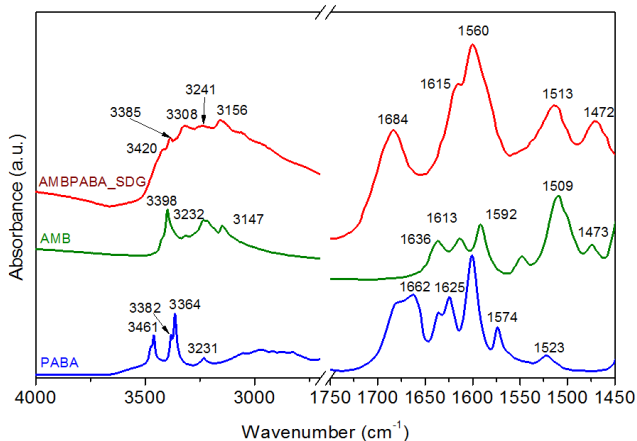


Figure 3.5.4. FTIR spectra for AMB, PABA and AMBPABA_SDG in 4000-1450 cm^{-1} spectral range.

Table 3.5.1. Frequencies vibration in IR for AMB and AMBPABA_SDG.

Spectral domain cm^{-1}	AMB cm^{-1}	AMBPABA_SDG cm^{-1}
3400–3200	~3398, 3232 NH ₂	~3420, 3385, 3308 NH ₂ ~3241 NH ₃ ⁺
3200 - 2700	~3147 NH	~3156 $\nu_{\text{NH}_2^+}$
1800–1500	~1636, 1613 NH ₂ or C=N ~1592 NH ₂	~1684, 1560 NH ₃ ⁺ $\delta_{\text{as-}}$, $\delta_{\text{as-}}$ ~1615 $\nu_{\text{NH}_2^+}$
1600–1500	~1509 NH	~1513 NH

3.5.4. ¹³C solid state NMR Spectroscopic

The ¹³C CP/MAS spectra of the AMB, PABA, and AMBPABA_SDG are shown in the Figure 3.5.5. The NMR spectra of AMB and PABA consist of eight, respectively six resonance lines, corresponding to the carbon sites in the molecular structure of these two compounds. From the comparison the ¹³C CP/MAS NMR spectra between AMB, PABA, AMBPABA_SDG, and the following conclusions can be drawn:

- (i) The ¹³C CP/MAS spectrum of the final compound (AMBPABA_SDG) is that it contains one molecule per asymmetric unit;
- (ii) The most significant difference which arises is a major AMB chemical shift displacement and line broadening especially for the C1 and C8 resonances;

¹³C solid-state NMR measurements are in concordance with PXRD conclusions regarding obtaining a new solid form.

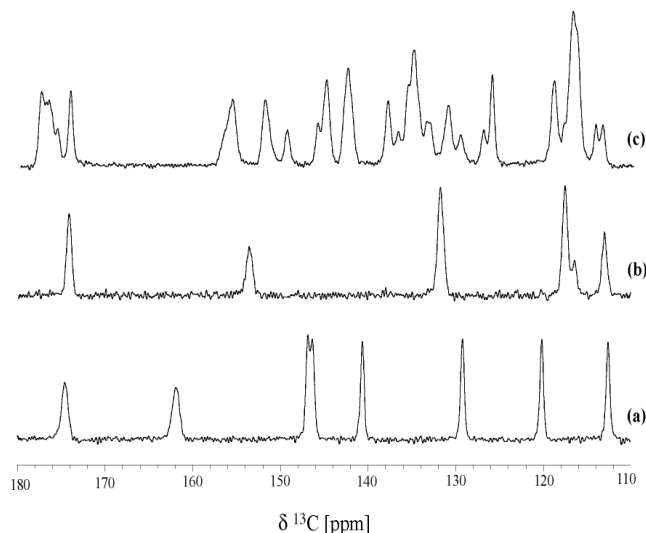


Figure 3.5.5. The ^{13}C CP/MAS NMR spectra of AMB (a), PABA (b), and AMBPABA_SDG (c), $\nu_R = 15$ kHz with and CP = 2 ms.

3.6. Ambazone with aspartatic acid

Aspartic acid $\text{C}_4\text{H}_7\text{NO}_4$ (ASP) is part of the amino acids class, is soluble in water and acts as an excitatory neuro-transmitter, as a generator of cellular energy and to stimulate increased production of immunoglobulins and antibodies. Aspartic acid has pKa values of: 1.88, 3.65, 9.60 and pKa value of ambazone is: 6.27, 7.37, 10.67, indicating the possibility of obtaining of salts. By SDG method were prepared two samples in 1:1 molar ratio of ambazone with aspartic acid at room temperature: one by grinding mixture of ethanol 5 minutes (AMBASP_SDG 5min) and the second sample grinding mixture of ethanol for 1 hour (AMBASP_SDG 1h).

3.6.1. DTA-TGA analyses

From the thermograms analysis obtained for the sample AMBASP_SDG (5 min) (Figure 3.6.1.a), an endothermic signal with maximum at 47°C appears which corresponds to 3.93 % mass loss, associated with water removal. In the range $180\text{-}220^\circ\text{C}$ exothermic signal is observed with maximum at 211°C with a mass loss of 30.23% phenomena associated to sample decomposition accompanied melting.

The DTA-TGA analysis obtained for sample AMBASP_SDG 1h (Figure 3.6.1.b), reveals an endothermic signal with maximum at 48°C which corresponds to 4.57% mass losses associated with removal of none bonded water. In the range $180\text{-}220^\circ\text{C}$, exothermic

signal is observed with maximum at 212°C and a mass loss of 30.6%, phenomenon associated with the sample decomposition accompanied melting.

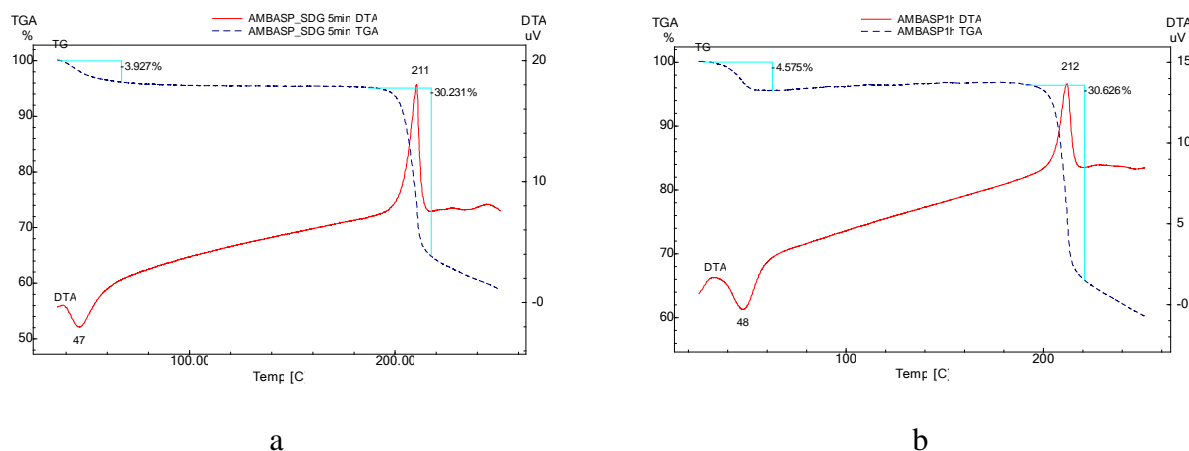


Figure 3.6.1. DTA-TGA of: AMBASP_SDG 5 min (a) and AMBASP_SDG 1 h (b).

3.6.2. Powder X-Ray Diffraction

Differences between PXRD patterns of AMB, ASP, AMBASP_SDG (5 min) and AMBASP_SDG 1h (Figure 3.6.2.) highlights two different solid forms for ambazone with aspartic acid. The two solid forms show that does not contain lines from ambazone or aspartic acid, thus proving relatively pure compounds obtained.

After indexing powder patterns for compound AMBASP_SDG 1 hour there were determined lattice parameters:

$$a = 21.37 \text{ \AA}, b = 6.09 \text{ \AA}, c = 8.55 \text{ \AA},$$

$$\alpha = 90^\circ, \beta = 96.65^\circ, \gamma = 90^\circ.$$

These compound crystallize in monoclinic system.

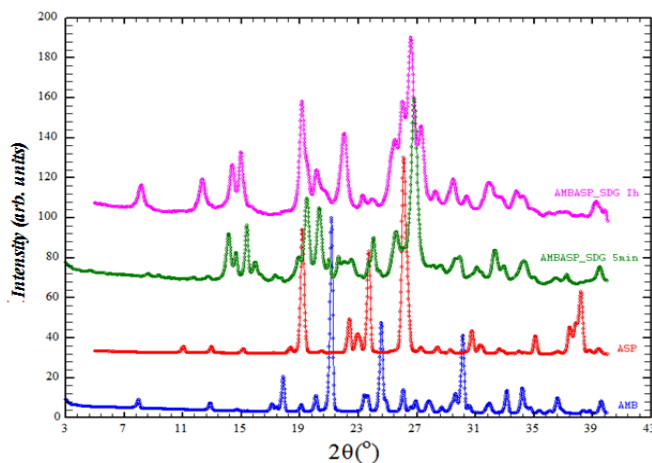


Figure 3.6.2. PXRD patterns for AMBASP_SDG 5min and AMBASP_SDG 1h.

3.6.3. Powder X-ray diffraction with variable temperature

In order to verify of results obtained by thermal analysis by X-ray diffraction with variable temperature in the 25-240°C range were performed (Figure 3.6.3.).

The powder patterns made on samples obtained by SDG 1 hour with variable temperature VTPXRD, shows the stability of AMBASP_SDG 1h to 198 °C temperature. Between 198 and 240 °C occurs the transition from amorphous phase to a crystalline phase. This result is in concordance with the DTA-TGA measurements, which are exothermic event at 212 °C, event attributed to decomposition overlapped with melting compound.

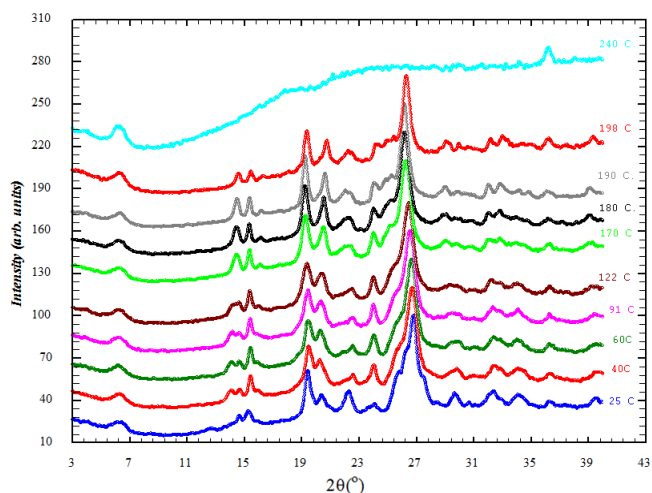


Figure 3.6.3 VTPXRD by AMBASP_SDG 1h, heated in the 25-240 °C temperature range.

3.6.4. Fourier Transformed Infrared Spectroscopy

The analysis of spectra obtained for compounds AMB, ASP și AMBASP_SDG 5 min, AMBASP_SDG 1h respectively (Figure 3.6.4.a,b) evidenced that the vibrations corresponding to amino-functional groups change in the case of compounds obtained by SDG for 5 minutes and one hour.

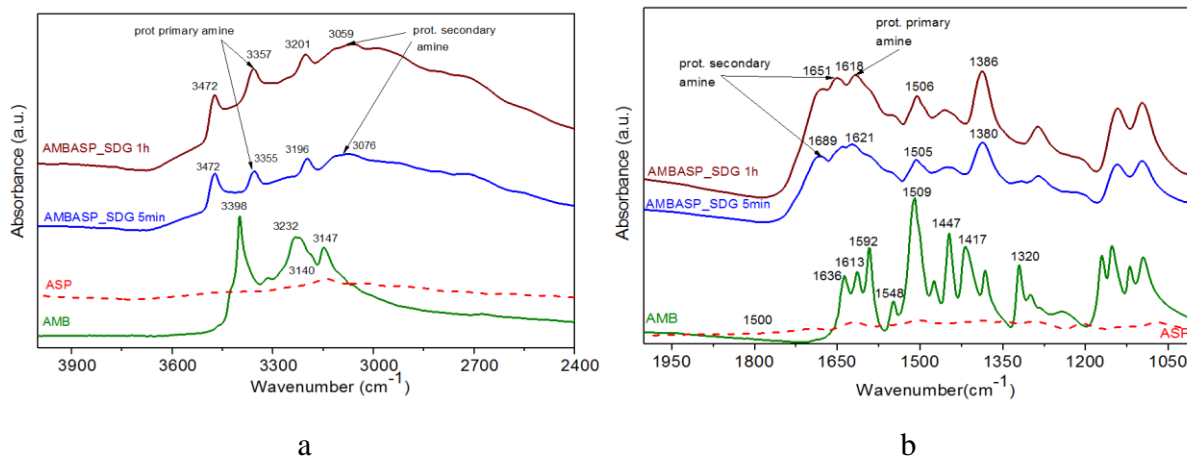


Figure 3.6.4. FTIR spectra of AMB, ASP and AMBASP_SDG 5 min, AMBASP_SDG 1h in 4000-2400 cm^{-1} (a), respectively 2000-1000 cm^{-1} (b) spectral range.

The primary amine vibration around 3398 cm^{-1} in the spectrum of AMB is shifted to higher value at $\sim 3472 \text{ cm}^{-1}$ in the spectra recorded for the compounds obtained by SDG method (AMBASP_SDG 5 min, AMBASP_SDG 1h respectively). Vibrations located around $\sim 3357 \text{ cm}^{-1}$ for AMBASP_SDG 5 min and $\sim 3355 \text{ cm}^{-1}$ for AMBASP_SDG 1h respectively, corresponds to protonated primary amines group NH_3^+ [Socrates 2001].

The vibration located at $\sim 3147\text{ cm}^{-1}$ in AMB spectrum is shifted in the spectrum of the compounds obtained by SDG 5 min and 1 hour at 3196 and 3201 cm^{-1} , which confirms the protonation of secondary amino-group for both compounds [Ivanova *et al* 2010]. New bands at ~ 3076 , 3059 cm^{-1} respectively can be attributed to the stretching vibration of the protonated secondary amine (NH_2^+) [Socrates 2001]. A broad bands of medium intensity at ~ 1689 and 1651 cm^{-1} of AMBASP_SDG 5min respectively AMBASP_SDG 1h can be assigned to deformation vibrations of the protonated secondary amine NH_2^+ . The medium intensity bands at ~ 1621 respectively 1618 cm^{-1} identified for the sample AMBASP_SDG 5min and AMBASP_SDG 1h correspond to deformation vibration of protonated primary amine NH_3^+ . These two new solid forms obtained with Ambazone aspartic acid, is justified by protonation of the secondary amines and shifts that occur in the spectra of the new compounds.

3.6.5. ^{13}C solid state NMR analysis

The solid state spectra ^{13}C NMR (Figure 3.6.5.) obtained for Ambazone and aspartic acid consist of eight and respectively six resonance lines. ^{13}C NMR spectra of AMBASP_SDG 5min and AMBASP_SDG 1h, have different resonance lines number compared with the ^{13}C NMR spectra of ambazone.

The solid state ^{13}C NMR spectrum of AMBASP_SDG 5min sample shows the appearance of a non-equivalence of aspartic acid in the network and we can conclude that most probably in the asymmetric unit exist two molecules of aspartic acid for one molecule of ambazone. On the other hand, the ^{13}C NMR spectrum of the solid state AMBASP_SDG 1 h shows that in this case exist one aspartic acid molecule for each Ambazone molecule into the asymmetric unit. Chemical shifts of resonance lines for AMB, ASP and two other samples prepared by SDG method are presented in Table 3.6.1.

Table 3.6.1. Chemical shifts ^{13}C CP/MAS NMR for AMB, ASP, AMBASP_SDG (5 min, 1 hour).

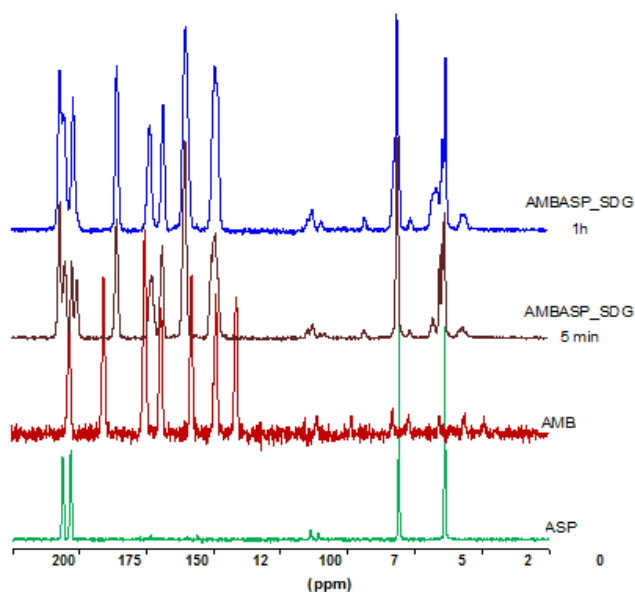


Figure 3.6.5. ^{13}C CP/MAS NMR spectra of AMB, ASP, (AMBASP_SDG 5 min) and (AMBASP_SDG 1h)

	δ AMB [ppm]	δ AMBASP_SDG 5min [ppm]	δ AMBASP_SDG 1h [ppm]	δ ASP [ppm]
Protonarea la inelul aromatic (C3, C4, C6, C7)	116.7 124.1 133.2 144.6	124.63 125.8 135.7x2	124.63x2 135.7x2	
Non-protonarea la inelul aromatic (C2, C5)	150.6 -	144.13 147.9	143.97 148.93	
C1,C8	165.8 178.7	161 180.2	161.2 180.8	
C9,C11		175.9 177.7 182.15	177.52 182.48	
C9		38.5 39.34 40.33	38.5 39.5	
C10		56.4	56.5 57.5	
C1a C2a C3a C4a C5a				25.6 27.7 54.4 177.8 178.8

3.7. Ambazone with nicotinic acid

Nicotinic acid (NA), with chemical formula $\text{C}_6\text{H}_5\text{NO}_2$ or vitamin B₃, is one of the essential human nutrients, water-soluble solid is a derivative of pyridine, is used as vasodilating medicines and in the treatment of diseases of the gastro-enteric tract [Makareyer *et al* 1997]. NA it present pKa of the aromatic ring N is 4.9 carboxyl group (-COOH) and pKa of the COOH group is 2.1 [Tim *et al* 1999]. Ambazone undergoes three protonation reactions with pK values at 10.69, 7.39 and 6.22 [Günter *et Hoffmann* 1990] and based on the fact that differences in pKa values for ambazone and nicotinic acid are large enough to allow the formation of salts, was prepared ambazona with nicotinic acid (NA) using SDG method. The Ambazone nicotinate (AMBNA_SDG) was prepared by grinding a mixture of 255.3 mg AMB and 123.11 mg NA with 1 ml twice distilled water added in drops in an agate mortar, at

room temperature, until a dried compound was obtained. The obtained solid form was characterized by thermal analysis DSC; DTA-TGA, X-ray powder diffraction and FTIR spectroscopy.

3.7.1. DSC, DTA-TGA analyses

Thermal analysis of AMB, NA and AMBNA_SDG are presented in Figure 3.7.1.a.

The thermal behavior of nicotinic acid presents an endothermic peak between 180–185°C, $\Delta H=1.66$ kJ/mol due probably to solid-solid transition and other sharp endotherm between 236–239°C, $\Delta H=27.92$ kJ/mol corresponding to the melt of compound followed by a small endothermic peak between 242–270°C due to the subliming of the nicotinic acid [Jingyan *et al* 2008]. The DSC curve for the AMBNA_SDG presents four signals: an endothermic peak between 80 and 115°C, with $\Delta H=32.37$ kJ/mol, corresponding to the loss of water molecules, an exothermic peak between 142 and 158°C, $\Delta H=11$ kJ/mol due probably to the solid-solid transition, an exothermic peak between 190 and 197°C with $\Delta H=31.61$ kJ/mol, followed by other exotherm event between 198–204°C, $\Delta H=6.44$ kJ/mol corresponding to the melting with decomposition of the sample.

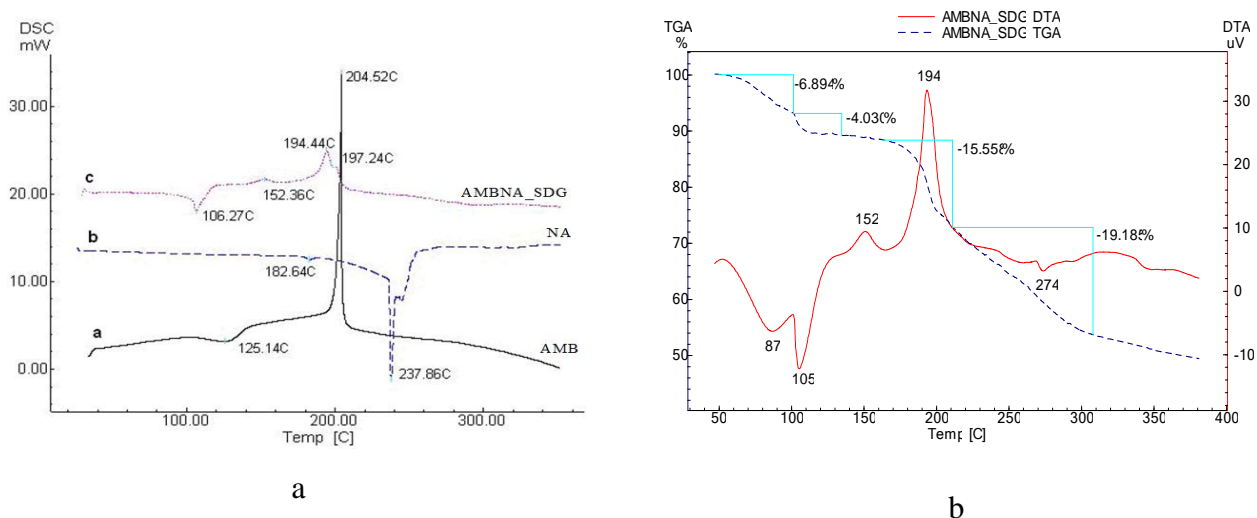


Figure 3.7.1. DSC traces for AMB, NA, AMBNA_SDG (a) and DTA-TGA thermograms for AMBNA_SDG (b).

DTA-TGA thermograms of AMBNA_SDG (Figure 3.7.1.b) indicate in the 60–100°C temperature range the first mass loss of 6.9 %, corresponding to a broad endothermic peak and another endotherm between 100 and 130°C with maximum at 106°C and mass loss of 3.8% due to the non-bonded and bonded water elimination. The third mass loss occurs between 180 and 210°C with loss of 15.6%, probably due to nicotinic acid subliming and

evaporation, and final in the range of 210–350°C, the mass loss of 19% occurs, corresponding to the elimination of volatile components which results by decomposition of ambazone and evaporation of the nicotinic acid. This step of mass loss corresponds to a sharp exotherm with T_{onset} at 175°C and peak maximum at 194°C. These signals have good similarity with DSC measurements.

3.7.2. Powder X-Ray Diffraction

The PXRD pattern of AMBNA_SDG (Figure 3.7.4.) is different as compared to those of AMB and NA ones. So, a new crystalline compound was obtained which belong to monoclinic system with the following unit cell parameters: $a=7.422 \text{ \AA}$, $b=40.439 \text{ \AA}$, $c=6.905 \text{ \AA}$, $\alpha=90^\circ$, $\beta=106.43^\circ$, $\gamma=90^\circ$.

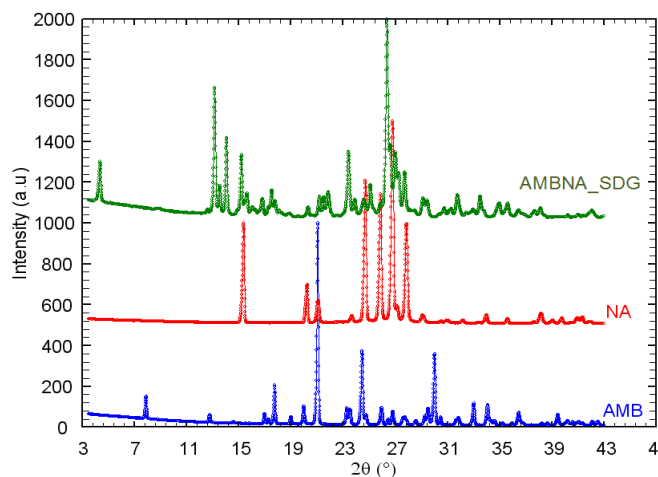


Figure 3.7.2. PXRD of AMB, NA and AMBNA_SDG

3.7.3. Fourier Transformed Infrared Spectroscopy

The characteristic peaks of nicotinic acid (Figure 3.7.3.a,b) can be recognized in the pure Nicotinic acid spectrum as to be: $\nu(\text{O-H})$ 3431 cm^{-1} , $\nu(\text{C-H})$ 3074 cm^{-1} , $\nu(\text{C=O})$ 1716 cm^{-1} , $\nu(\text{C=C})$ $1595\text{--}1416 \text{ cm}^{-1}$, $\delta(\text{C-H})$ (in-plane) $1183\text{--}1039 \text{ cm}^{-1}$ [Jingyan *et al* 2008]. The band at $\sim 3400 \text{ cm}^{-1}$ can be assigned to N–H stretching of primary amine in pure ambazone (Figure 3.7.3.a), it can be also observed as a shoulder in the spectrum of AMBNA_SDG. The salt formation has been shown to modify the NH stretching absorption in amines [Socrates 2001]; it was observed that the free bases have a sharp strong band at $\sim 3226 \text{ cm}^{-1}$ due to the NH stretching and that this band is greatly reduced in intensity in the spectra of the AMBNA_SDG. The band at 3146 cm^{-1} corresponds to the NH vibration [Socrates 2001] for pure AMB, it identify in salt spectrum at 3164 cm^{-1} can be assigned to N–H stretching of secondary amine. A new shoulder appeared at $\sim 2970 \text{ cm}^{-1}$ probably due to the protonated secondary amine.

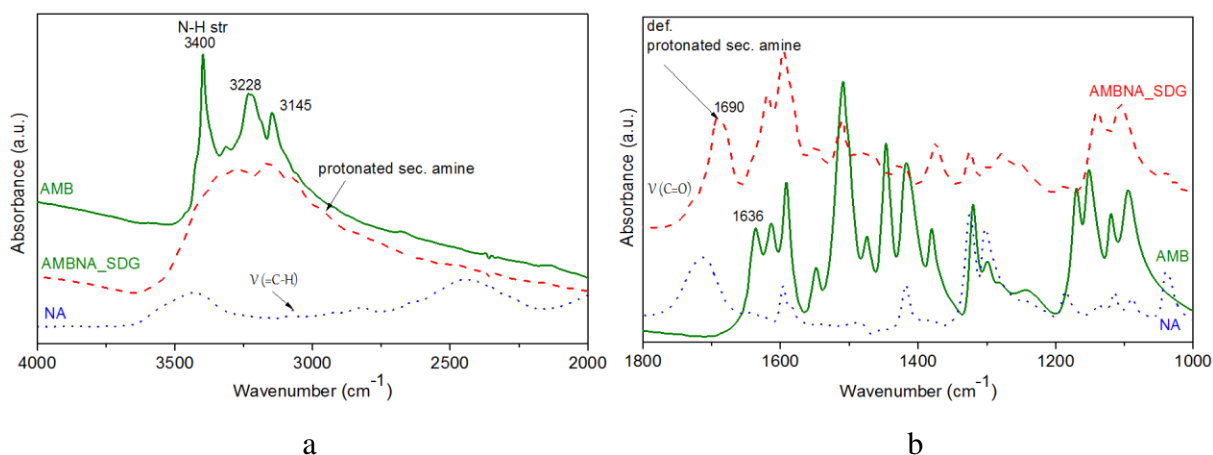


Figure 3.7.3. FTIR spectra of AMB, NA and AMBNA_SDG in 4000-2000 cm^{-1} (a) and 1800-1000 cm^{-1} (b) spectral range.

Primary amine has an absorption band of medium intensity at $\sim 1613 \text{ cm}^{-1}$ (Figure 3.7.3.b.), being located at $\sim 1618 \text{ cm}^{-1}$ by salt formation [Socrates 2009]. Pure ambazone spectrum contains the secondary amine vibration at 1508 cm^{-1} which is not shifted in AMBNA_SDG spectrum. In the spectrum of the salt a new strong absorption appeared at $\sim 1692 \text{ cm}^{-1}$, which is assigned to deformation vibration of the protonated secondary amino group [Muresan-Pop *et al* 2011a,b]. This frequency is not present in the FTIR spectrum of pure AMB, *i.e.*, a salt was formed between ambazone and nicotinic acid.

3.8. Ambazone with lactic acid

The Lactic acid, $\text{C}_3\text{H}_6\text{O}_3$ (2-hydroxypropanoic acid) (LA), is a chemical compound that plays an important role in various biochemical processes; it is able to release energy for the resynthesize of ATP without oxygen involvement, the process is called anaerobic glycolysis. The Lactic Acid belongs to the group of weak hygroscopic acids containing alcohol in the position Alpha in the group carboxylic [Siegfried 1995]. The sample AMBLA_SDG was prepared by grinding a mixture of 255.3 mg AMB and 0.086 ml LA to fill up 1 ml with twice distilled water added in drops in an agate mortar at room temperature, until a dried compound was obtained (SDG method).

3.8.1. DSC, DTA-TGA analyses

The DSC curves of the pure AMB and of the compound obtained by solvent drop grinding between AMB and LA are presented in Figure 3.8.1.a. The thermal behavior of aqueous solution of LA presents two endothermic events with maximums at 119 and 126°C , due to water elimination, respectively to the sublimation of the compound. DSC curve of AMBLA_SDG presents two events: a small broad endothermic peak between 100 and 140°C ,

with a maximum at 125°C corresponding to the loss of water molecules and an exothermic event between 170 and 200°C, with maximum at 182°C due to the sample decomposition.

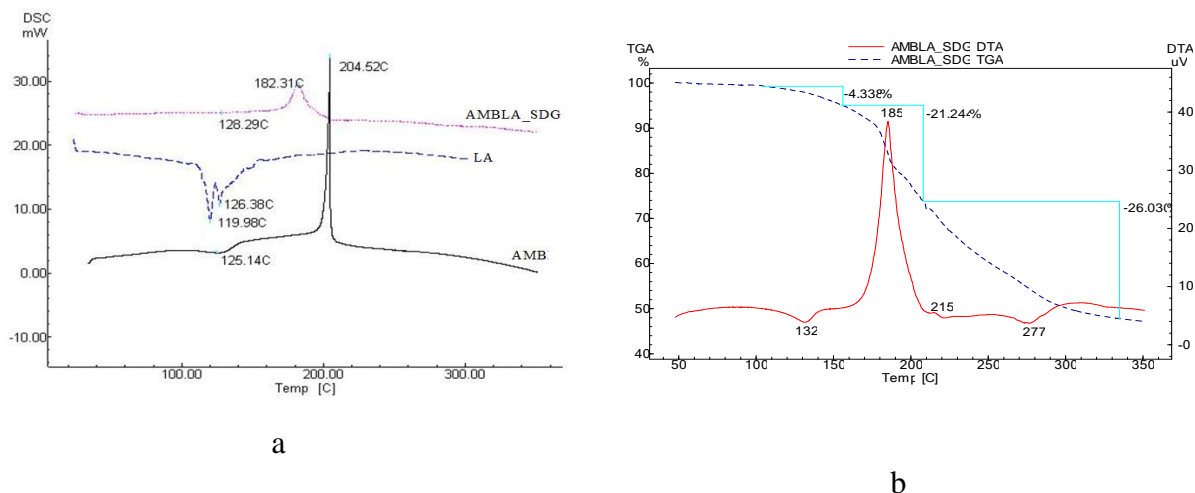


Figure 3.8.1. DSC traces of AMB; LA, and AMBLA_SDG (a); DTA-TGA thermograms of AMB and AMBLA_SDG (b).

Simultaneous DTA-TGA measurements for AMBLA_SDG (Figure 3.8.1.b) indicates in the 100–140°C temperature range the first mass loss of 4.4%, corresponding to a small broad endothermic peak with maximum at 132°C. The second mass loss occurs between 140 and 210°C with a loss of 21%, probably due to lactic acid subliming and corresponds to a sharp exotherm with a maximum at 185°C. The final mass loss of 26% occurs in the range of 210–330°C and corresponds to the elimination of volatile components which results by decomposition of ambazone and evaporation of the lactic acid. The difference between the characteristic temperatures of the pure samples and of the AMBLA_SDG shows the formation of a new compound.

3.8.2. Powder X-Ray Diffraction

The powder patterns for AMB and AMBLA_SDG (Figure 3.8.2.) are different; this indicates the formation of a new solid form. The compound obtained was included and found to crystallize in the triclinic system with the following network parameters: $a=10.781\text{Å}$, $b=9.352\text{Å}$, $c=7.348\text{Å}$, $\alpha=93.65^\circ$, $\beta=92.14^\circ$, $\gamma=98.15^\circ$.

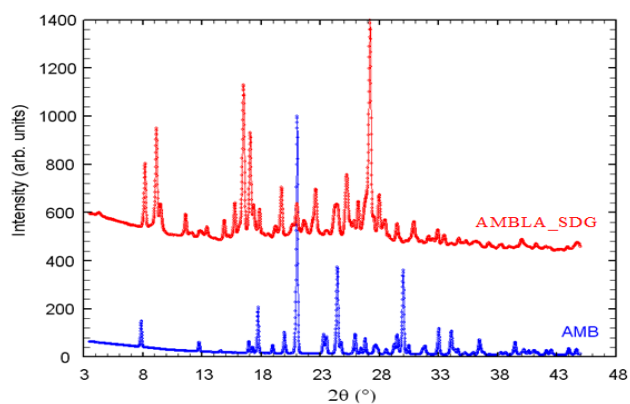


Figure 3.8.2 PXRD of AMB and AMBLA_SDG.

3.8.3. Fourier Transformed Infrared Spectroscopy

The band at $\sim 3400\text{ cm}^{-1}$ can be assigned to N–H stretching from primary amine in pure ambazone; it can be observed also as a shoulder in the spectrum of AMBLA_SDG (Figure 3.8.3.a.).

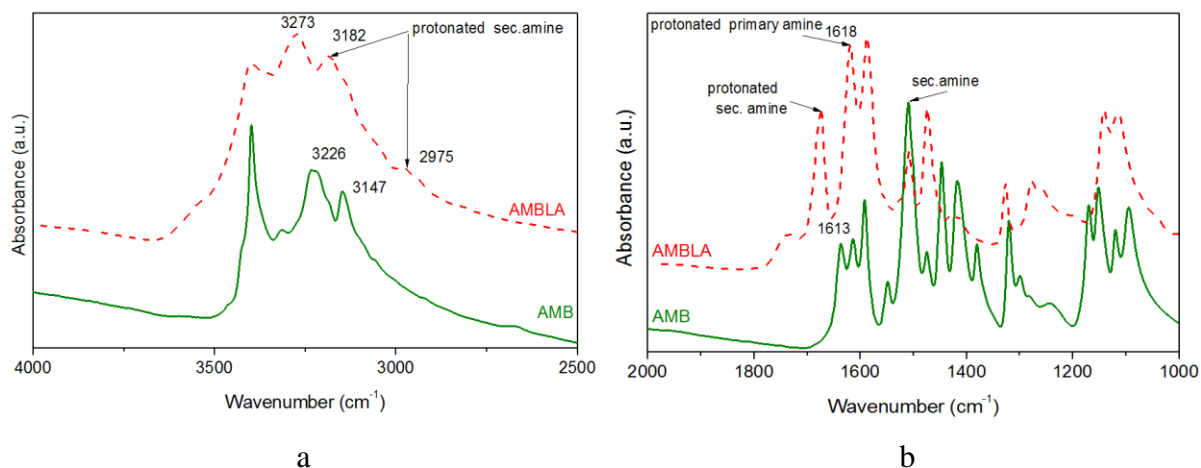


Figure 3.8.3. FTIR spectra of AMB and AMBLA_SDG in 4000–2500 cm^{-1} (a) and 2000–1000 cm^{-1} (b) spectral range.

Salt formation has been shown to modify the NH stretching absorption in amines [Socrates 2001]; it was observed at 3273 cm^{-1} a signal reduced in intensity in the spectrum of the AMBLA_SDG compared with the ambazone one. The band at 3146 cm^{-1} for AMB which corresponds to the N-H stretching vibration of secondary amine [Socrates 2001] is shifted at 3182 cm^{-1} in salt spectrum. A new shoulder appeared at $\sim 2975\text{ cm}^{-1}$ probably due to the protonated secondary amine.

Primary amine has an absorption band of medium intensity at $\sim 1613\text{ cm}^{-1}$ (Figure 3.8.3.b), being located at $\sim 1618\text{ cm}^{-1}$ by salt formation [Socrates 2009] correlated with NH stretching vibration. The pure ambazone spectrum contains the secondary amine vibration at 1508 cm^{-1} which is not shifted in AMBLA_SDG spectrum, but greatly reduced in intensity. In the spectrum of the salt a new strong absorption band appeared at $\sim 1676\text{ cm}^{-1}$, which is assigned to deformation vibration of the protonated secondary amino group NH_2^+ . This frequency is not present in the FTIR spectrum of pure AMB, *i.e.*, a salt was formed between ambazone and lactic acid [Muresan-Pop *et al* 2011a].

Based on the FTIR spectrum of AMBLA_SDG the occurrence of the characteristic frequencies of the NH_2^+ group indicates a salt formation between AMB and LA by proton transfer.

CHAPTER 4

4. Conclusions, original contributions, publications, perspectives

4.1. General conclusions

During this research, there have been prepared and investigated a large number of biologically active compounds based on Ambazone. These compounds are new solid forms of Ambazone obtained and characterized for the first time.

The following conclusions had been drawn:

1. Depending on the solvent which had been used, through some recrystallization procedures we could established the conditions for the anhydrous Ambazone to transform into monohydrate Ambazone and reversely. Through DTA-TGA, FTIR, NMR analysis and powder X-Ray Diffraction method, it was revealed the different behaviour of anhydrous Ambazone in comparison with the monohydrate form. Using variable temperature X-ray Powder Diffraction on monohydrate Ambazone it was pointed out that: up to 90°C remains the monohydrate form, between 90-125°C it becomes anhydrous form, between 125-185°C the anhydrous form holds, between 185-198°C the anhydrous form disappears and at 210°C it decomposes. These results are in agreement with the thermal analysis.

2. Monocrystal of Ambazone monohydrate was obtained and its crystal structure was resolved by X-ray single-crystal diffraction; the compound crystallizes in the monoclinic system having the space group $P2_1/c$, with a molecule per asymmetric unit. There were determined the unit cell's parameters and the atoms positions in the unit cell. Consequently, the distances between atoms, bond angles and hydrogen bonds were obtained. Further on, the anhydrous Ambazone single crystal was obtained and its crystal structure was determined. It was established that the compound crystallize in monoclinic system, having the space group $P2_1$, with two molecules per asymmetrical unit. The unit cell parameters and the atoms positions into the unit cell were determined. From the atoms position in the unit cell there were obtained the distances between atoms, bond angles and hydrogen bonds.

3. Three different solid forms of ambazone were prepared by various methods, using acetic acid. Powder X-ray diffraction, thermal and spectroscopic methods revealed that the

obtained Ambazone compounds are salts. By the variable temperature powder X-ray diffraction, for the solid form of Ambazone with acetic acid obtained through SDG in 1:1 molar ratio, the temperature up to which the compound is stable was found to be 100°C; above this temperature, the transformation into amorphous phase takes place. By the powder X-ray diffraction and indexing procedure of the other two forms obtained by Ambazone with acetic acid, it was established that both of them crystallized in the monoclinic system, one of them having the space group C2, and the other one C2/c. There were also determined the lattice parameters for these solid forms.

4. Ambazone acetate single-crystals were also prepared using the vapor diffusion method. The crystal structure was determined by X-ray single-crystal diffraction, and it was established that this compound crystallizes in monoclinic system, having the space group C2/c, with one Ambazone molecule and two acetic acid molecules per asymmetric unit. There were determined the lattice parameters, atoms positions into the unit cell, distances and bond angles, and it was pointed out inter and intra-molecular hydrogen bonds.

5. It was obtained a new solid form of Ambazone with hydrochloric acid it was proved its formation. FTIR, RMN and thermal analyses have shown that this new compound is a salt. By indexing of powder patterns, results that the new compound crystallizes in the monoclinic system, having the space group $P_{21/c}$ with four ambazone molecules and four chlorine atoms per unit cell.

6. Another resulted salt was Ambazone with glutamic acid. DTA, DTA-TGA analyses revealed the differences between Ambazone and the new compound thermal behavior. By FT-IR the protonation at amino groups in Ambazone structure were identified, thus establishing the salt character of the compound. By powder patterns indexing it was concluded that the resulted salt crystallizes in the monoclinic system having the space group P_{21} , two Ambazone and two glutamic acid molecules per asymmetric unit. This conclusion was also sustained by solids state NMR analysis.

7. From Ambazone with p-aminobenzoic acid it resulted a new solid form that was also investigated through thermal methods, spectroscopic analyses (FTIR and NMR), leading to the conclusion that the Ambazone salt with p-aminobenzoic acid was formed. By powder diffraction patterns indexing it resulted that the crystallographic system of the compound is triclinic and the lattice parameters were obtained.

8. Using SDG method, Ambazone with aspartic acid was prepared, resulting two different solid forms, considering different preparation time, five minutes and one hour

respectively. For both samples the thermal behavior was analyzed by DTA-TGA. Using powder X-ray diffraction on sample obtained by SDG one hour it was shown that the crystallization system is monoclinic and the lattice parameters were obtained. FTIR measurements on pure Ambazone and SDG resulting compounds attest the obtaining of Ambazone salt with aspartic acid. Variable temperature diffraction measurements for the compound obtained by SDG one hour, demonstrated its stability up to 198°C, this result being in agreement with the thermal measurements. The solids state NMR analysis pointed out that the new compound obtained from SDG 5 minutes has two aspartic acid for one Ambazone molecule in the asymmetric unit, while the compound obtained by SDG one hour compound has one aspartic acid molecules at one Ambazone molecule in the asymmetric unit.

9. From Ambazone with lactic acid it was prepared a new compound that was also investigated through DSC, DTA-TGA methods, being established the thermal behavior, different from that of pure Ambazone. FT-IR method revealed the protonation of the amine group, thus resulted the salt feature of the compound. Using the powder X-ray diffraction it was established that crystallographic system is triclinic and the lattice parameters were obtained.

10. Starting from Ambazone and nicotinic acid it was obtained a new solid form which was investigated through DSC, DTA-TGA; the thermal behavior was different from that of pure Ambazone. As a result of FTIR analysis, it was established that a protonation at the secondary amine group from Ambazone structure takes place, meaning that a salt is being formed. By indexing the powder diffraction pattern of the compound it resulted that it crystallizes in the monoclinic system and the lattice parameters were determined.

4.2. Original contributions

As a synthesis of the research results there are the following conclusions:

- ❖ There were obtained 11 new solid forms from Ambazone;
- ❖ These were characterized through PXRD, thermal methods (DSC, DTA-TGA), spectroscopic methods (FTIR, NMR);
- ❖ There were obtained three single-crystals: for the hydrous and anhydrous form of Ambazone and for Ambazone with acetic acid;
- ❖ It was determined the complete crystalline structure for the three single-crystals.

Bibliografie selectivă

- [Amlacher *et al* 1990a] Amlacher R, Baumgart J, Hartl A, Weber H, Kuhnel HJ, Schulze W, Hoffmann H, Arch Geschwulstforsch 60 (1990) 11–8.
- [Baumgart *et al* 1990] Baumgart J, Gase K, Schulze W, Suehnel J, Gutsche W, Behnke D, Cancer Lett. 54 (1990) 119-24.
- [Bernstein 2006] Bernstein J, Polymorphism and Patents from a Chemist's Point of View, în Polymorphism în the pharmaceutical industry, Wiley-VCH, Weinheim, (2006) 365–82.
- [Bond 2007] Bond AD, Cryst Eng Comm 9 (2007) 833-834.
- [Brittain 2009] Brittain HG, Polymorphism în pharmaceutical solids, (Drugs and the Pharmaceutical Sciences), Second Edition Informa Healthcare USA Inc.52 Vanderbilt Avenue New York, NY 10017, 192 (2009).
- [Chakrapani *et al* 2008] Chakrapani H, Wilde TC, Citro ML, Goodblatt MM, Keefer LK, Saavedra JE, Bioorg. & Med. Chem., 16 (2008) 2657–64.
- [Etter *et al* 1993] Etter MC, Reutzel SM, Choo CG, J Am Chem Soc 115 (1993) 4411-12.
- [Fichtner *et al* 1983] Fichtner I, Arnold W, Pharmazie, 38(2) (1983) 130–1.
- [Gomes *et al* 2001] Gomes JANF, Mallion RB, Chem Rev 101 (2001) 1349–84.
- [Günter *et al* 1990] Gunter L, Hoffmann H, Biophysical Chemistry (1990) 287-300.
- [Ivanova *et al* 2010] Ivanova B and Spitteller M, Spectrochim. ActaA 77 (2010) 849–855.
- [Jingyan *et al* 2008] Jingyan S, Jie L, Yun D, Ling H, Xi Y, Zhiyong W, Yuwen L and Cunxin W, JTAC 93 (2008) 403–9.
- [Koleva *et al* 2009] Koleva BB, Kolev T, Seidel RW, Spitteller M, Mayer-Figge H and Sheldrick WS, J Phys ChemA, 113 3088–95 (2009).
- [Kuhnel *et al* 1988a] Kuhnel HJ, Amlacher R, Baumgart J, Schulze W, Arch Geschwulstforsch 58 (1988) 217–22.
- [Löber *et al* 1990] Löber G and Hoffmann H, Biophys Chem 35 (1990) 287–300.
- [Makareyer *et al* 1997] Makareyer EN, Makedonov Yu V and Lozorskaya EL, Russian Chemical Bulletin 46 (1997).
- [Mocuta *et al* 2008] Mocuta H, Borodi G, Simon S, 3rd International Conference Advanced Spectroscopies on Biomedical and Nanostructured Systems”, 7-10 sept Babes-Bolyai University Cluj-Napoca (2008).
- [Mureşan-Pop *et al* 2011a] Mureşan-Pop M, Kacsó I, Tripon C, Moldovan Z, Borodi Gh, Bratu I and Simon S, J. Therm. Anal. Calorim. 104 (2011) 299–306.
- [Mureşan-Pop *et al* 2011b] Mureşan-Pop M, Kacsó I, Filip X, Vanea E, Borodi G, Leopold N, Bratu I, Simon S, Spectroscopy, 26 (2011) 115-28.
- [Otsuka *et al* 1994] Otsuka M, Otsuka K, Kaneniwa N, Drug Dev Ind Pharm 20 (1994) 1649–60.
- [Petersen *et al* 1955] Petersen S, Gauss W, Urbschat E, Angew. Chem. 67 (1955), on line (2006) 217-231.
- [SDBS 2007] Spectral Database for Organic Compounds SDBS (<http://riodb01.ibase.aist.go.jp>) SDBS 1097 (2007).
- [Siegfried 1995] Siegfried RW, Drug Cosmet Ind 156 (1995) 30-37 104-105.
- [Socrates 2001] Socrates G, Infrared and Raman Characteristic Group Frequencies: Tables and Charts, 3rd edn, Wiley, West Sussex 332 (2001) 107-13 222-24 332.
- [Stilinic *et al* 2008] Stilinic V, Cincik D and Kaitner B, Acta Chim Slov 55 (2008) 874–79.
- [Tim *et al* 1999] Tim KY and Takacs, Novak K, Pharm Res 16 (1999) 377-81.

MULȚUMIRI

Doresc să-i mulțumesc în mod special coordonatorului științific al acestei lucrări, D-nului Prof. Univ. Dr. Simion Simon, pentru îndrumarea, sprijinul și valoroasele cunoștințe științifice oferite pe parcursul întregul program doctoral.

Mulțumiri grupului de cercetători de la INCDTIM din Cluj-Napoca: Dr. Irina Kacso, Tehn. Sorina Ciupe, Dr. G. Borodi și Dr. I. Bratu, pentru valoroasa colaborare din acești ani.

Mulțumesc colaboratorilor de la Universitatea din Bologna, departamentul “Molecular Crystall Engineering Group, G. Ciamician” Prof. Univ. Dr. Dario Braga, Prof. Univ. Dr. Fabrizia Grepioni, Dr. Lucia Maini din Bologna, pentru sprijinul acordat în cadrul experimentelor de creștere de monocristale.

De asemenea, îmi exprim mulțumirea față de toți colegii din cadrul Institutului de Cercetări Experimentale și Interdisciplinare ICEI (Cristina, Oana, Emilia, Adriana, Monica, Diana, Zsolt, Mihai) care mi-au oferit deopotrivă suport științific și sprijin moral.

Mulțumiri speciale față de cei care au condus proiectul POSDRU 6/1.5/S/3 – “Doctoral Studies: Through Science Towards Society” Babeș-Bolyai University, Cluj-Napoca, Romania, pentru finanțarea acordată în cei trei ani de studiu.

Și nu în ultimul rând,

Mulțumesc părinților mei, fiicei mele Isabelle, surorilor și prietenei mele Iulia Miclăuș, pentru susținerea și încurajările pe care mi le-au dat în acești ani.